CIRANO
Knowledge into action

COPULA-BASED ESTIMATION OF HEALTH CONCENTRATION CURVES WITH AN APPLICATION TO COVID-19

TAOUFIK **BOUEZMARNI**
MOHAMED **DOUKALI**
ABDERRAHIM **TAAMOUTI**

2022s-07
WORKING PAPER

CS

CIRANO
Knowledge into action

Center for Interuniversity Research and Analysis on Organizations

The observations and viewpoints expressed in this publication are the sole responsibility of the authors; they do not necessarily represent the positions of CIRANO or its partners. *Les idées et les opinions émises dans cette publication sont sous l'unique responsabilité des auteurs et ne représentent pas nécessairement les positions du CIRANO ou de ses partenaires.*

ISSN 2292-0838 (online version)

Copula-based estimation of health concentration curves with an application to COVID-19

Taoufik Bouezmarni[*], *Mohamed Doukali*[†] *and Abderrahim Taamouti*[‡]

March 22, 2022

Abstract

COVID-19 has created an unprecedented global health crisis that caused millions of infections and deaths worldwide. Many, however, argue that pre-existing social inequalities have led to inequalities in infection and death rates across social classes, with the most-deprived classes are worst hit. In this paper, we derive semi/non-parametric estimators of Health Concentration Curve (HC) that can quantify inequalities in COVID-19 infections and deaths and help identify the social classes that are most at risk of infection and dying from the virus. We express HC in terms of copula function that we use to build our estimators of HC. For the semi-parametric estimator, a parametric copula is used to model the dependence between health and socio-economic variables. The copula function is estimated using maximum pseudo-likelihood estimator after replacing the cumulative distribution of health variable by its empirical analogue. For the non-parametric estimator, we replace the copula function by a Bernstein copula estimator. Furthermore, we use the above estimators of HC to derive copula-based estimators of health Gini coeffcient. We establish the consistency and the asymptotic normality of HC's estimators. Using different data-generating processes and sample sizes, a Monte-Carlo simulation exercise shows that the semiparametric estimator outperforms the smoothed nonparametric estimator, and that the latter does better than the empirical estimator in terms of Integrated Mean Squared Error. Finally, we run an extensive empirical study to illustrate the importance of HC's estimators for investigating inequality in COVID-19 infections and deaths in the U.S. The empirical results show that the inequalities in state's socio-economic variables like poverty, race/ethnicity, and economic prosperity are behind the observed inequalities in the U.S.'s COVID-19 infections and deaths.

Keywords/Mots-clés: Health concentration curve, Gini coeffcient, inequality, copula, semi/non-parametric estimators, COVID-19 infections and deaths / Courbe de concentration de la santé, coefficient de Gini, inégalité, copule, estimateurs semi-/non paramétriques, infections et décès COVID-19

JEL Codes/Codes JEL: C13, C14, I14

Pour citer ce document / To quote this document

Bouezmarni T., Doukali M. and Taamouti A. (2022). Copula-based estimation of health concentration curves with an application to COVID-19 (2022s-07, CIRANO).
https://doi.org/10.54932/MTKJ3339

[*] Département de MathÈmatiques, UniversitÈ de Sherbrooke, CIREQ, CREAS. TaouÖk.Bouezmarni@USherbrooke.ca

[†] McGill University and Centre Interuniversitaire de Recherche en Analyse des Organisations (CIRANO). Department of Economics, McGill University, Leacock Building, 855 Sherbrooke Street West, Montreal, Quebec H3A 2T7, Canada. mohamed.doukali@mail.mcgill.ca

[‡] Corresponding author. Department of Economics, University of Liverpool Management School. Address: Chatham St, Liverpool L69 7ZH. Abderrahim.Taamouti@liverpool.ac.uk

1 Introduction

COVID-19 has created an unprecedented global health crisis that caused millions of deaths worldwide. However, many argue that pre-existing social inequalities led to inequalities in the number of infections and deaths across social classes, with the most-deprived classes are worst hit. In a 2020 report on unequal risks of infection and severe illness, World Health Organization (WHO) European Region pointed out that COVID-19 exposure risk and the severity of its health, social and economic impacts are not being felt equally.[1] Thus, given the devastating impact of the pandemic and to address the above health inequities, policymakers are urged to identify those classes that are most at risk of infection and dying from the virus and set containment measures to deal with these inequities in COVID-19's infections and deaths. In this paper, we aim to develop new estimation approaches that can help detect health inequalities that are caused by different socioeconomic factors such as poverty, race, etc. These estimation techniques will be used to check if real data on COVID-19's infection and deaths supports the claims regarding the impact of socioeconomic factors on COVID-19 exposure risk and deaths.

Chen and Krieger (2021) argue that reporting disaggregated COVID-19 cases by race/ethnicity and socioeconomic position is vital to informing efforts to distribute resources, develop treatments, and coordinate public policy. They point out that "*As of May 6, 2020, tables on the US Centers for Disease Control and Prevention's (CDC's) own Web page reporting COVID-19 cases by race/ethnicity indicated that 54.2% of reported cases were missing race/ethnicity information.*" Using data from Public Health Disparities Geocoding Project [see Krieger et al. (2003, 2005), Krieger et al. (2002, 2003a,b)], Chen and Krieger (2021) uses descriptive statistics to report disparities in COVID-19 death rate in the US by county level sociodemographic attributes using available surveillance and US Census data. Furthermore, Chin, et al. (2020) report that preliminary data from the epidemic in the US show that demographic and socioeconomic issues make low-income communities and people of color more vulnerable to COVID-19 than others. To assess each county's level of risk of high COVID-19 medical burden, Chin, et al. (2020) examine available data for a range of characteristics for all U.S. counties, or county equivalents.

Moreover, Knittel and Ozaltun (2020) use both linear regression and negative binomial mixed models to study the correlation between county-level COVID-19 death rates and some socio-economic variables across states as well as within states. Their analysis shows that across states higher shares

[1] See the WHO's report here: https://apps.who.int/iris/bitstream/handle/10665/338199/WHO-EURO-2020-1744-41495-56594-eng.pdf

of African American and elderly residents are correlated with higher death rates. However, this correlation becomes statistically insignificant within a given state, while remaining positive. They also find that a higher share of people not working, that counties with higher home values, higher summer temperatures, and lower winter temperatures are correlated with higher death rates. Furthermore and unexpectedly, they do not find a correlation between poverty rates, pollution or obesity rates and death rates. Using linear regressions models and monthly county-level mortality data, McLaren (2021) studies the socio-economic roots of racial disparities in COVID-19 mortality. After controlling for state-level effects, he shows that there is a strong positive correlation across counties between the minority's population share and COVID-19 deaths. However, he also finds that for Asian-Americans the correlation is fragile, and disappears when one controls for some variables like education, occupation, and commuting patterns. McLaren (2021) argues that regardless of what other factors are controlled for, the racial disparity in mortality rates cannot be explained by differences in income, poverty rates, education, occupational mix, or even access to healthcare insurance. For other empirical studies on the impact of socioeconomic variables on COVID-19 infections and deaths for other countries other than the U.S., the readers can consult Ehlert (2021), Bermudi et al. (2021), Lassale et al. (2020) among others.

Using a theoretical model, Brown and Ravallion (2020) incorporate within-county median incomes, poverty, income inequality, age, and racial composition to model the social distancing responses to the threat of catching COVID-19 and outcomes for infections and deaths across U.S. counties. For the empirical implementation of the model, they use regressions to show that there is a statistically significant effect of socioeconomic covariates on social distancing and infections, but not on deaths. Furthermore, they find that richer counties tend to see greater gains in social distancing and lower infection rates, and that income poverty and inequality tend to increase the infection rate, but these effects are largely accountable to their correlation with racial composition.

None of the above-mentioned studies, however, use proper measures of health that are designed to detect inequalities in COVID-19's infections and deaths across social classes. These studies are based on simple correlations and regressions, which might not help quantify inequalities in infections and deaths. To measure health inequality based on socioeconomic variables, Wagstaff et al. (1989) introduced a concentration index that takes into consideration a specific weight function that represents the aversion to socioeconomic health inequality. This concentration index could be viewed as an extension of the Gini index, which is widely adopted in the income inequality literature. Since the work of Wagstaff et al. (1989), several alternative indices based on concentration curves have been established by using different weight functions that represent different judgements of inequality aversion, see Wagstaff et al. (1991), Wagstaff (2002, 2005), Allison and Foster (2004), Erreygers and Van Ourti (2011), Zheng (2011) among others.

In this paper, we use copula functions to develop semiparametric and nonparametric estimators of health concentration curves that are designed to quantify health inequalities. These estimators will be applied to study inequalities in COVID-19's infections and deaths across U.S. states as well as within these states (counties). Health concentration curves allow us to obtain plots of cumulative percentage of the health variable (e.g. COVID-19's infection rate and COVID-19's death rate) against the cumulative percentage of the population, ranked by socio-economic covariates such as living standards (beginning with the poorest and ending with the richest), race, etc. These plots help to visualize easily inequalities in health variables by observing the position of the health concentration curve with respect to 45-degree line (known as the line of equality) in a two-dimensional space. If each individual in the dataset had equal chance of contracting/dying from COVID-19 regardless of their socioeconomic position, then as we move from lowest socioeconomic position to highest socioeconomic position, the proportion of individuals with/died of COVID-19 should remain the same, and in this case the health concentration curve matches the 45-degree line, otherwise we say that there is inequality not in favour of individuals with lowest socioeconomic position (if the curve is above the 45-degree line) or not in favour of individuals with highest socioeconomic position (if the curve is below the 45-degree line). The farther the curve is above/below the line of equality, the more concentrated the COVID-19's infections/deaths is among the individuals with lowest socioeconomic position/highest socioeconomic position, respectively.

We first show that the dependence structure between health and socioeconomic variables is crucial for the estimation of health concentration curves. We re-formulate the health concentration curve as a function of copula and derive expressions for HC for some specific copula functions. In particular, we consider the independence case and lower and upper Fréchet–Hoeffding dependence structures. The latter type of dependence helps illustrate the link between health concentration curve and Lorenz curve of the health variable of interest.

Next, we use the above-mentioned copula-based re-formulation to develop semi-parametric and nonparametric estimators of health concentration curves. To derive the semi-parametric estimator, a parametric copula function is used to model the dependence between health and socio-economic variables. The parameter of the copula function is estimated using the maximum pseudo-likelihood estimation technique after replacing the cumulative distribution of health variable (or the argument of copula function) by its nonparametric analogue (empirical distribution function). Once the maximum likelihood estimator of the copula's parameter is obtained, we use it to calculate the semi-parametric estimator of health concentration curve. For the non-parametric estimator of the health concentration curve, we replace the copula function by its smoothed non-parametric estimator, which we obtain using Bernstein copula. Bernstein estimator helps avoid the misspecification problem that might face the semiparametric estimator. Furthermore, we use the above estimators of the health concentration curve to derive semi-parametric and nonparametric estimators of health Gini coefficient.

Moreover, we study the asymptotic properties of the above estimators. We establish their consistency and asymptotic normality. We provide expressions for their variances, which might be used to construct confidence intervals and build tests for health concentration curve and health Gini coefficient. Using different data-generating processes and sample sizes, a Monte-Carlo simulation exercise shows that the semiparametric estimator outperforms the smoothed nonparametric estimator, and that the latter does better than the empirical estimator in terms of Integrated Mean Squared Error. Furthermore, we run an extensive empirical study to illustrate the importance of our estimators for quantifying and investigating inequality in COVID-19's infections and deaths in the U.S. Our empirical results show that effectively some socio-economic variables like poverty, race, and economic prosperity of a state might explain the observed inequalities in COVID-19's infections and deaths.

The rest of this paper is organized as follows. In Section 2, we introduce the notations, reformulate the health concentration curve as a function of copula and derive its expression for some specific copula functions. In Section 3, we develop semi-parametric and nonparametric estimators of health concentration curve using parametric and non-parametric copulas, which in turn use to derive estimators of Gini health index. In Section 4, we study the asymptotic properties of the semiparametric and nonparametric estimators. In Section 5, we run Monte Carlo simulations to assess the performances of the semiparametric and nonparametric estimators and compare them with the one of the classical empirical estimator of the concentration health. Section 6 contains an extensive empirical study using our estimators and U.S. COVID-19 data and Section 7 concludes. The proofs of the theoretical results can be found in the Appendix.

2 Copula-based health concentration curve

The health concentration curve plots the cumulative percentage of the health variable against the cumulative percentage of the population, ranked by socio-economic covariates such as living standards, beginning with the poorest and ending with the richest. The curve illustrates the effect of a socio-economic variable on concentration of a health variable such as COVID-19 infection or death. Formally, consider H representing the health variable of interest and Y a socio-economic random variable such as income. Let f be the joint density of the vector (H, Y), with f_H and f_Y the marginal densities of H and Y, $f_{H|Y}$ the conditional density of H given Y, and F_H and F_Y the marginal distributions of H and Y. For $p \in (0,1)$, the health concentration curve is defined as

$$CH(p) = \frac{\int_0^p \mathbb{E}\left[H \mid Y = F_Y^{-1}(u)\right] du}{\int_0^1 \mathbb{E}\left[H \mid Y = F_Y^{-1}(u)\right] du}, \tag{1}$$

where, for $u \in (0,1)$, $F_Y^{-1}(u) = \inf\{t : F_Y(t) \geq u\}$ is the quantile function of Y. The values of $F_Y^{-1}(u)$ at $u = 0$ and $u = 1$ can be set to arbitrary finite real numbers. For example, if Y is the income and H is the rate of COVID-19 mortality, $CH(p)$ is the percentage of the cumulative rate of COVID-19 mortality rate of the $100p\%$ of the poorest population.

Observe now that the structure of the dependence between H and Y plays a crucial role in the calculation of health concentration curve $CH(p)$. For instance, if H and Y are independent, then $CH(p) = p$, i.e., we are in the presence of perfect equality of health variable H across the socio-economic variable Y. However, this does not mean a perfect equality of the health concentration. As shown in the following proposition, the concentration health curve can be derived through dependence structure of the vector (H, Y) using copula function [see the proof of Proposition 1 in the appendix].

Proposition 1 *Let C and c be the copula function and the copula density function of the vector (H, Y), respectively. The health concentration curve (CH) in Equation (1) can be rewritten as a function of copula:*

$$CH(p) = \frac{\int_0^1 F_H^{-1}(u) C_u(u,p) du}{\mathbb{E}(H)}, \text{ for } p \in (0,1), \tag{2}$$

where $C_u(u,p)$ is the partial derivative of the copula function of the vector (H, Y) :

$$C_u(u,v) = \frac{\partial C(u,v)}{\partial u} = \int_0^v c(u,z) dz.$$

The result in (2) is a copula-based representation of CH. We now use this representation to derive expressions of the health concentration curve for some specific copula functions. We consider the independence case and the Fréchet–Hoeffding lower and upper bounds of copula. As shown below, the latter dependence structures help illustrate the link between the concentration curve and the Lorenz curve of the health variable H.

Example 1 (Independence): *If H and Y are independent, then $C_u(u,v) = v$. Therefore, $CH(p) = p$, and in this case we obtain a perfect equality, i.e. the socio-economic variable has no effect on the concentration of the health variable.*

Example 2 (Lower Fréchet–Hoeffding): Suppose that H and Y are countermonotonic random variables, i.e., the dependence between the two variables can be modelled using the Fréchet–Hoeffding lower bound copula $W(u,v) = \max\{u+v-1, 0\}$. In this case, $W_u(u,p) = \mathbb{I}(u > 1-p)$, where $\mathbb{I}(.)$ is an indicator function that takes the value one if $u > 1-p$ and zero otherwise. Hence,

$$CH(p) = \frac{\int_0^1 F_H^{-1}(u) W_u(u,p) du}{\mathbb{E}(H)} = \frac{\int_{1-p}^1 F_H^{-1}(u) du}{\mathbb{E}(H)} = 1 - L_H(1-p),$$

where L_H is the Lorenz curve of H. For example, if H represents overweightness, then $CH(p)$ is the percentage of the total overweightness of the $100p\%$ of the richest population.

Example 3 (Upper Fréchet–Hoeffding): Suppose that H and Y are comonotone random variables, i.e., the dependence between the two variables can be modelled using the Fréchet–Hoeffding upper bound copula $M(u,v) = \min\{u,v\}$. In this case, $M_u(u,p) = \mathbb{I}(u < p)$, where $\mathbb{I}(.)$ is an indicator function that takes the value one if $u < p$ and zero otherwise. Hence,

$$CH(p) = \frac{\int_0^1 F_H^{-1}(u) M_u(u,p) du}{\mathbb{E}(H)} = \frac{\int_0^p F_H^{-1}(u) du}{\mathbb{E}(H)} = L_H(p),$$

For example, if H represents the payments people made for health care and if we assume a perfect positive correlation between income Y and H, then $CH(p)$ is the percentage of the total payments spent by the $100p\%$ of the poorest population.

3 Estimation of copula-based Health concentration curve

In this section, the copula-based representation of CH in (2) will be used to derive semi-parametric and nonparametric estimators of health concentration curve and Gini coefficient. For the semi-parametric estimator, we consider a parametric copula function to model the dependence between health and socio-economic variables. The parameters of the copula are estimated using the maximum pseudo-likelihood estimator after replacing the cumulative distribution of health variable by its empirical analogue. For the non-parametric estimator, we replace the copula function by the Bernstein copula estimator. Furthermore, we use the previous estimators to derive semi-parametric and nonparametric estimators of health Gini coefficient.

Let us first set some notations. We denote by $\{(H_i, Y_i), i = 1, \ldots, n\}$ an independent and identically distributed sample of n copies of the vector (H, Y). From the representation in (2), we see that the health concentration curve can be estimated using different approaches that represent different ways of estimating the expectation and distribution of the health variable H, say $\mathbb{E}(H)$ and F_H, but also the ways we estimate the copula function $C_u(u,p)$. In the following, $\mathbb{E}(H)$ is estimated using its empirical analogue (sample average of H) and F_H is estimated using the rescaled empirical distribution:

$$\widehat{F}_H(h) = \frac{1}{n+1} \sum_{i=1}^{n} \mathbb{I}(H_i \le h), \tag{3}$$

where $\mathbb{I}(.)$ is an indicator function that takes the value one if $H_i \leq h$ and zero otherwise. Note that alternative estimators of F_H - such as a parametric estimator or a smooth nonparametric estimator (Kernel, Bernstein, etc.) - can be considered.

Regarding the estimation of copula function, in the next sub-sections we consider two different estimators of $C_u(u,p)$. In Sub-section 3.1, we introduce a semiparametric estimator of $CH(p)$ in which only realizations of Y in $C_u(u,p)$ will be used for estimating the copula function, i.e., the information on Y are required for modelling the dependence structure of the random vector (H,Y). In Sub-section 3.2, we derive the nonparametric estimator of $CH(p)$ using a nonparametric estimator (hereafter Bernstein estimator) of copula $C_u(u,p)$.

3.1 Semiparametric estimation

Suppose now that the copula C of (H,Y) belongs to a parametric family of copulas $\{C(.,.,\theta), \theta \in \Theta\}$, with an unknown vector parameter θ that is in the set Θ a compact subset of $\mathbb{R}^q$. Denote by θ_0 the true value of the parameter θ. There exist several estimators of θ_0 and the most popular one is given by the following maximum pseudo likelihood estimator:

$$\hat{\theta}_n = \underset{\theta}{\operatorname{argmax}} \sum_{i=1}^{n} \log c\left(\widehat{F}_H(H_i), \widehat{F}_Y(Y_i), \theta\right), \tag{4}$$

where c is the copula density of C, $\widehat{F}_H(h)$ is defined in (3) and $\widehat{F}_Y(y) = (n+1)^{-1}\sum_{i=1}^{n} \mathbb{I}(Y_i \leq y)$. Note that $\widehat{\theta}_n$ is the estimator proposed by Shih and Louis (1995) and Genest, Ghoudi and Rivest (1995). The asymptotic representation of $\widehat{\theta}_n$ can be obtained from the proof of Theorem 1 in Tsukuhara (2005).

Using the maximum likelihood estimator of θ_0 in (4) and the nonparametric estimator of F_H in (3), a semiparemetric estimator of $CH(p)$ can be obtained as follows:

$$\widehat{CH}(p) = \frac{\sum_{i=1}^{n} H_i \, C_u(\widehat{F}_H(H_i), p, \widehat{\theta}_n)}{\sum_{i=1}^{n} H_i}, \tag{5}$$

where $C_u(u,v,\theta) = \frac{\partial C(u,v,\theta)}{\partial u}$. Next, we use the examples in Section 2 to illustrate the semiparametric estimator of $CH(p)$ in (5). We also compare the latter estimator with the following empirical estimator of $CH(p)$ [see Wagstaff (2002)],

$$\widehat{CH}_n(p) = \frac{\sum_{i=1}^{n} H_i \mathbb{I}(Y_i \leq \widehat{F}_Y^{-1}(p))}{\sum_{i=1}^{n} H_i}, \tag{6}$$

where $\mathbb{I}(.)$ is an indicator function that takes the value one if $Y_i \leq \widehat{F}_Y^{-1}(p)$ and zero otherwise. The results are reported in Figure 1 that we obtain after generating $n = 100$ observations of (H_i, Y_i) from a Gaussian copula with correlation coefficients $\rho = 0$ (Example 1), $\rho = -0.99$ (close to Example 2) and $\rho = 0.99$ (close to Example 3), and from marginal distributions of H and Y that are given by the exponential distribution with a parameter $\lambda = 1$. To avoid numerical problems, we excluded the cases $\rho = \pm 1$. Thereafter, we report the results for both known and unknown copula function. When the latter is unknown, we use the R package `VineCopula` to select the copula that better fits the generated data [see the curves unknown copula in the sub-figures of Figure 1]. Figure 1 also illustrates estimators of $1 - L_H(1-p)$ and $L_H(p)$ - see subfigures (b) and (c) of Figure 1 that correspond to Examples 2 and 3 -, where L_H denotes the Lorenz curve of H.

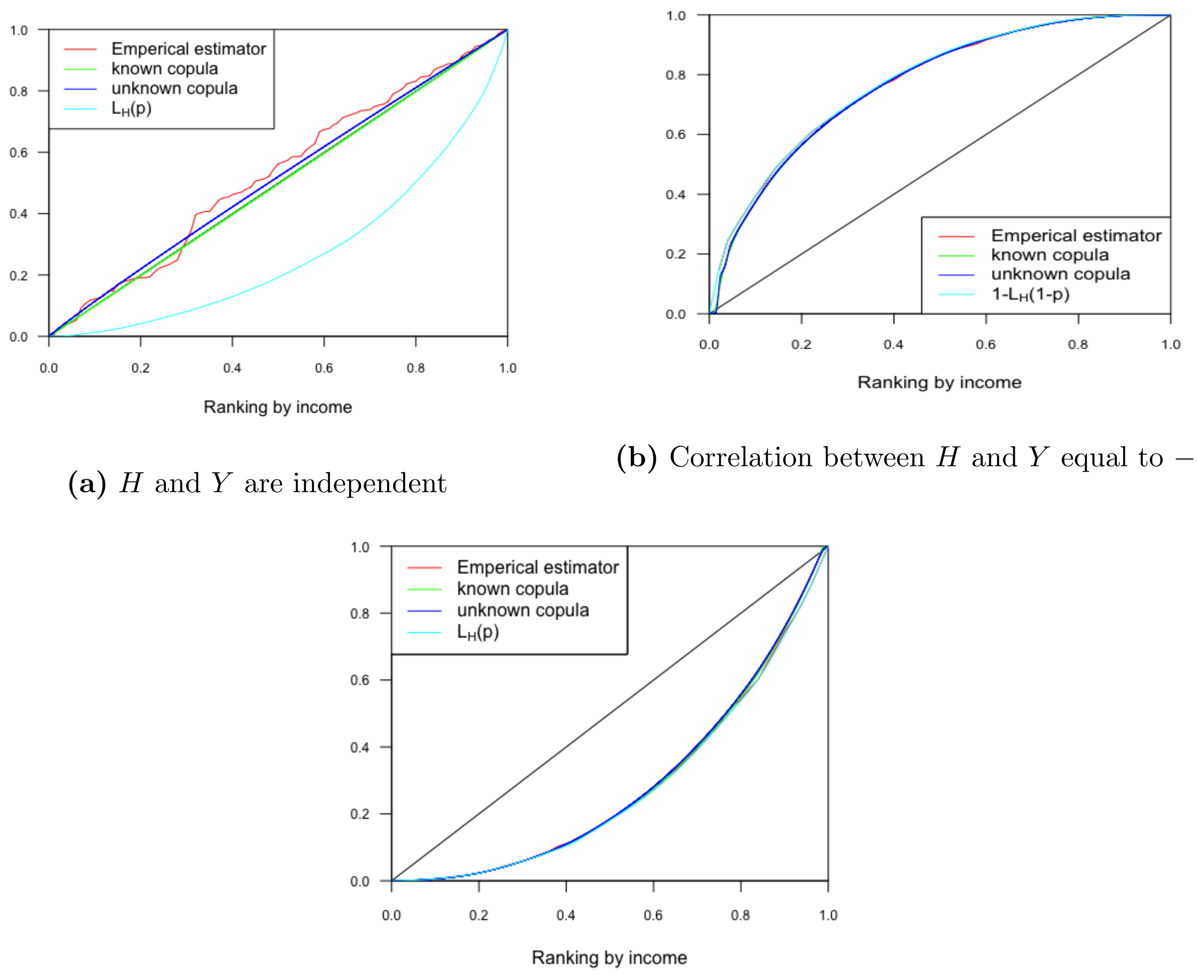

(a) H and Y are independent

(b) Correlation between H and Y equal to -0.99

(c) Correlation between H and Y equal to 0.99

Figure 1: *This figure illustrates the copula-based semiparametric estimator and the empirical estimator of the health concentration curve $CH(p)$ for different structures of dependence between H and Y.*

Subfigure (a) of Figure 1 shows that the copula-based estimator of $CH(p)$ is much closer to the

45-degree line (true curve of $CH(p)$ under independence) than the empirical estimator, and that the former is also much smoother than the latter. This result holds for both known and unknown copulas, which might indicate a high performance in favour of our semi-parametric estimator. We see that the estimators of $CH(p)$ for known and unknown copulas are very close, which might indicate that the R package `VineCopula` we use to select the copula function performs well. Moreover, we find that the Lorenz curve's estimator of H is quite far from the 45-degree line, which suggests that perfect equality using $CH(p)$ does not imply perfect equality using L_H. Subfigures (b) and (c) illustrate the semiparametric and empirical estimators of $CH(p)$ and of $1-L_H(1-p)$ (or L_H) when the dependence between H and Y is given by lower and upper Fréchet–Hoeffding, respectively. From these subfigures, we see that the estimators of $CH(p)$ and $1-L_H(1-p)$ are quite close, but again our semi-parametric estimator is smoother than the empirical estimator of $CH(p)$.

3.2 Nonparametric estimation

The semiparametric estimation approach of CH assumes that the copula function C of (H, Y) belongs to a parametric family of copulas. In practice, however, the copula's family is unknown, thus the semiparametric estimator in (5) can be biased if the used parametric copula is misspecified. To overcome this issue, we propose a nonparametric estimation of CH based on the following nonparametric estimator of copula (Bernstein copula). Formally, we consider the following Bernstein estimator of $C(u, v)$:

$$C_{m,n}(u,v) = \sum_{k_0=0}^{m} \sum_{k_1=0}^{m} C_n\left(\frac{k_0}{m}, \frac{k_1}{m}\right) P_{m,k_0}(u) P_{m,k_1}(v), \tag{7}$$

where m is an integer that plays the role of bandwidth, C_n is the empirical copula, and

$$P_{m,k}(z) = \left(\begin{array}{c} m \\ k \end{array}\right) z^k (1-z)^{m-k},$$

is the binomial distribution function with the parameters (m, k). For independent and identically distributed ($i.i.d.$) data, Sancetta and Satchell (2004) introduced a Bernstein polynomial estimator of the copula function and established the asymptotic normality of the Bernstein density copula. Sancetta and Satchell (2004) show that, under some regularity conditions, any copula function can be approximated by a Bernstein copula. Moreover, asymptotic properties of the Bernstein density copula for α-mixing data are studied in Bouezmarni et al. (2010). Janssen et al. (2012) have shown that the Bernstein copula outperforms the classical empirical copula originally proposed by Deheuvels (1979). Furthermore, an estimator of the partial derivative $C_u(u, v)$ can be derived using the Bernstein copula, but not the empirical copula.

Using the Bernstein copula in (7), a nonparametric estimator of the first-order partial derivative of the copula function, $C_u(u,p)$, can be obtained as follows:

$$\widetilde{C}_u(u,p) = m \sum_{k_0=0}^{m-1} \sum_{k_1=0}^{m} \left[C_n\left(\frac{k_0+1}{m}, \frac{k_1}{m}\right) - C_n\left(\frac{k_0}{m}, \frac{k_1}{m}\right) \right] P_{m-1,k_0}(u) P_{m,k_1}(p). \tag{8}$$

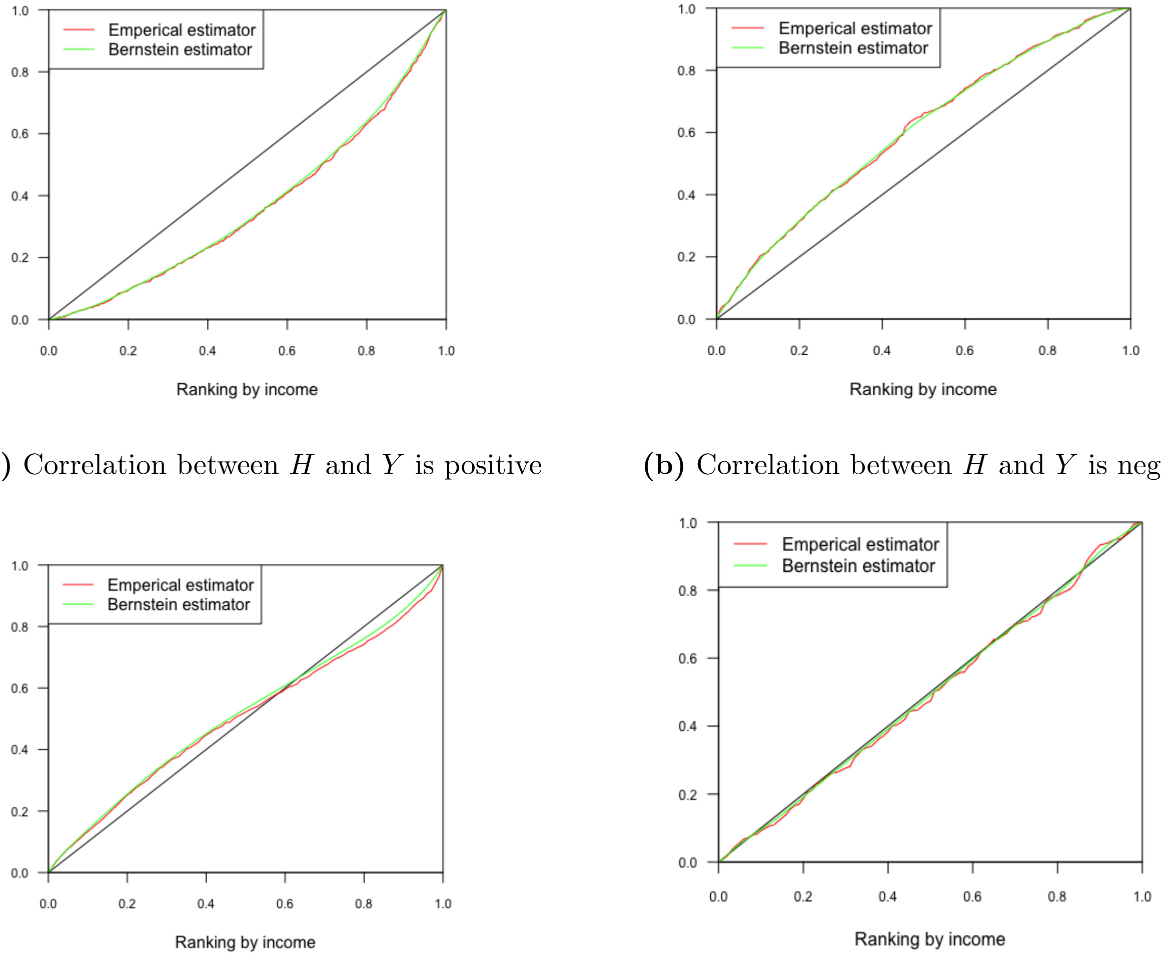

(a) Correlation between H and Y is positive

(b) Correlation between H and Y is negative

(c) Correlation between H and Y changes sign

(d) H and Y are independent

Figure 2: *This figure illustrates the Bernstein copula-based estimator and the empirical estimator of the health concentration curve $CH(p)$ for different degrees of dependence between H and Y.*

This estimator was introduced and its asymptotic properties were derived in Janssen et al. (2016). From (2) and (8), a nonparametric estimator of $CH(p)$ can be defined as follows:

$$\widehat{CH}_{m,n}(p) = \frac{\sum_{i=1}^{n} H_i \, \widetilde{C}_u(\widehat{F}_H(H_i), p)}{\sum_{i=1}^{n} H_i} \tag{9}$$

We now use some examples of dependence between H and Y to illustrate the nonparametric estimator in (9). For this, we generate $n = 100$ observations of (H_i, Y_i) using a Gaussian copula with correlation coefficients: (a) $\rho = 0.6$, (b) $\rho = -0.6$, (c) dependence between H and Y is quadratique, and (d) $\rho = 0$ (independence). The results reported in Figure 2 shows that the Bernstein copula-based estimator outperforms the empirical estimator as it is much closer to the 45-degree line in the case of independence - under which the true curve of $CH(p)$ matches the 45-degree line - and it is much smoother for the other cases of dependence.

3.3 Gini health index estimation

We now use the previously developed estimators of CH to propose estimators of Gini health index. This index is a measure of dispersion intended to quantify the health inequality within a socioeconomic group. Formally, the Gini health index is defined as follows:

$$G = 2\int_0^1 (p - CH(p))\, dp = 2\frac{Cov(H, F_Y(Y))}{\mathbb{E}(H)}. \tag{10}$$

Observe that under independence between H and Y, the covariance between H and $F_Y(Y)$ is equal to zero, and therefore the Gini health index G is equal to zero. The index G takes values between -1 and 1. A negative value of G indicates a pro-poor health, and in this case the health concentration curve will be above the 45-degree line; see Subfigure 1(b). A positive value of G indicates a pro-rich health, and in this case the health concentration curve is below the 45-degree line; see Subfigure 1(c). The Gini health index G is equal to zero when the concentration curve is close to the 45-degree line, see Subfigure 1(a). However, notice that the Gini health index - which is equal to the integral of the difference between the 45-degree line and the curve $CH(p)$ - can be equal to zero even when the health concentration curve does not coincide with the 45-degree line as shown in Subfigure 2(c). Thus, $CH(p)$ curve should represent a better way of visualizing and detecting health inequalities.

If H and Y are comonotone random variables - i.e., the dependence between the two variables can be modelled using the upper Fréchet–Hoeffding -, then $CH(p) = L_H(p)$ and G represents a Gini health coefficient constructed from Lorenz curve. In this case, we have $F_H(H) = F_Y(Y)$ and $G = \frac{2}{\mathbb{E}(H)}Cov(H, F_Y(Y)) = \frac{2}{\mathbb{E}(H)}Cov(H, F_H(H))$. Formally,

$$G = 2\int_0^1 (p - CH(p))\; dp = 2\int_0^1 (p - L_H(p))\, dp.$$

If H and Y are countermonotonic random variables - i.e., the dependence between the two variables can be modelled using the lower Fréchet–Hoeffding -, then $CH(p) = 1 - L_H(1-p)$ and G will be equal to minus Gini health index calculated based on Lorenz curve L_H. Formally,

$$G = 2\int_0^1 (p - CH(p))\; dp = 2\int_0^1 (p - 1 + L_H(1-p))\, dp{=} - 2\int_0^1 (p - L_H(p))\, dp$$

Formally, we can show that G is equal to minus Gini health coefficient based on Lorenz curve by observing that $F_H(H) = 1 - F_Y(Y)$ and $Cov(H, F_Y(Y)) = -Cov(H, F_H(H))$.

Now, using the expression of G in Equation (10) and the estimators of $CH(p)$ in Equations (5) and (9), we propose the following semiparametric

$$\widehat{G} = 2\int_0^1 \left(p - \widehat{CH}(p)\right)\, dp \tag{11}$$

and nonparametric

$$\widetilde{G} = 2\int_0^1 \left(p - \widehat{CH}_{m,n}(p)\right)\, dp$$

estimators of Gini health index, respectively.

We next establish the asymptotic properties of the semiparametric and nonparametric estimators of the health concentration curve CH. These properties can be used to establish the asymptotic properties of the estimators of the Gini health index.

4 Asymptotic properties of the estimators of CH

We investigate the consistency and asymptotic normality of the previously developed estimators of health concentration curve CH. Subsections (4.1) and (4.2) state the asymptotic i.i.d. representations of the semiparametric and nonparametric estimators $\widehat{CH}(p)$ and $\widehat{CH}_{m,n}(p)$ in (5) and (9), respectively.

4.1 Asymptotic properties of semiparametric estimator of CH

In this section, we assume that the copula function C belongs to a known parametric family of copulas $\mathcal{C} = \{C(.;\theta), : \theta \in \Theta\}$, where Θ is a compact subset of $\mathbb{R}^q$. Let $\hat{\theta}_n$ be an estimator of the true parameter θ_0 that satisfies the following condition:

Assumption A: *The estimator $\hat{\theta}_n$ of θ_0 satisfies:*

$$\hat{\theta}_n - \theta_0 = n^{-1}\sum_{i=1}^{n}\xi_i + o_p(n^{-1/2}), \tag{12}$$

where $\xi_i = \xi(F_H(H_i), F_Y(Y_i); \theta_0)$ is a q-dimensional random vector such that $E(\xi) = 0$ and $E\left(||\xi||^2\right) < \infty$, with $||.||$ represents the Euclidean norm.

Note that the estimators of θ_0 that have been proposed in Shih and Louis (1995) and Genest, Ghoudi and Rivest (1995) satisfy Assumption **A**. Tsukuhara (2005) also provides the asymptotic representation of $\widehat{\theta}_n$ and establishes some asymptotic properties of this estimator.

Now, before we state the asymptotic representation of the semiparametric estimator of CH, we need to introduce the following notations:

- $C_{uu} = \dfrac{\partial^2 C}{\partial u^2}$ and $C_{u,\theta} = \left(\frac{\partial C_u}{\partial \theta_1}, \ldots, \frac{\partial C_u}{\partial \theta_q}\right)$.
- $r_\theta(p, \theta) = \left(\frac{\partial\, r(p,\theta)}{\partial \theta_1}, \ldots, \frac{\partial\, r(p,\theta)}{\partial \theta_q}\right)^\top$ where $r(p,\theta) = \mathbb{E}\left[H C_u(F_H(H), p, \theta)\right].$

Using the above notations, we consider the following additional assumptions that we need in order to establish the result in Theorem 1.

Assumption B: We assume that:

B1: (i) $\mathbb{E}|H| < \infty$ and **(ii)** $hF_H(h) \to 0$ as $h \to -\infty$**;**

B2: $C_{u,u}$ and $C_{u,\theta}$ are continuous on $(0,1)^2$ and $(0,1) \times \Theta$, respectively;

B3: $\mathbb{E}[H\, C_{u,u}(F_H(H), p; \theta_0)]^2 < \infty$;

B4: $\mathbb{E}[H\, \frac{\partial C_u}{\partial \theta_k}(F_H(H), p; \theta_0)]^2 < \infty$, $k = 1, \ldots, q$.

The following theorem states the asymptotic i.i.d. representation of the semiparametric estimator $\widehat{CH}(p)$ in (5) [see the proof of Theorem 1 in the Appendix].

Theorem 1 *Under Assumptions **A**, **B1-B4**, we have*

$$\widehat{CH}(p) - CH(p) = n^{-1} \sum_{i=1}^{n} \zeta_i + o_p(n^{-1/2}),$$

where,

$$\zeta_i = \mathbb{E}(H)^{-1} \left[H_i C_u(F_H(H_i), p, \theta_0) + \xi_i^\top r_\theta(p, \theta_0) + \eta(H_i, p, \theta_0) - H_i\, CH(p)\right]$$

with $\eta(H_i, p, \theta_0) = \mathbb{E}_H\left[H\left(\mathbb{I}(H_i \leq H) - F_H(H)\right) C_{uu}(F_H(H), p, \theta)\right], r_\theta(p, \theta_0) = \mathbb{E}\left[H\, C_{u,\theta}(F_H(H), p, \theta_0)\right],$ ξ_i *is defined in Assumption **A**,* $\mathbb{E}_H$ *represents expectation with respect to* H, *and* $\mathbb{I}(.)$ *is an indicator function that takes value one if* $H_i \leq H$ *and zero otherwise.*

Notice that Theorem 1 can be used to establish the asymptotic normality of the semiparametric estimator $\widehat{CH}$ with zero mean and asymptotic variance:

$$Var(\widehat{CH}(p)) = \mathbb{E}\left(\zeta_i^2\right) - \left(\mathbb{E}(\zeta_i)\right)^2,$$

where the expression of ζ_i is defined in Theorem 1. This variance is unknown, but it can be estimated by replacing the unknown quantities in the expressions of $\mathbb{E}(\zeta_i)$ and $\mathbb{E}\left(\zeta_i^2\right)$ by their empirical analogues. However, for testing and building confidence interval around $\widehat{CH}(p)$, we recommend to use bootstrap.

4.2 Asymptotic properties of nonparametric estimator of CH

We now establish the asymptotic i.i.d representation of the nonparametric estimator of CH. First, let us define some new terms. For independent random vectors $(U_1, V_1), \dots, (U_n, V_n)$, with joint distribution function C, we define

$$W_{i,m}(u,v) = m \sum_{k_0=0}^{m-1} \sum_{k_1=0}^{m} \left[A_i(k_0,k_1) - A_i(k_0,m) C_u(u,v) \right] P_{m-1,k_0}(u) P_{m,k_1}(v),$$

where

$$A_i(k_0,k_1) = \mathbb{I}\left(\frac{k_0}{m} < U_i \leq \frac{k_0+1}{m}, V_i \leq \frac{k_1}{m} \right) - P\left(\frac{k_0}{m} < U_i \leq \frac{k_0+1}{m}, V_i \leq \frac{k_1}{m} \right).$$

The following theorem states the asymptotic i.i.d. representation of the nonparametric estimator $\widehat{CH}_{m,n}(p)$ in (9) [see the proof of Theorem 2 in the Appendix].

Theorem 2 *Suppose that the second derivatives* $C_{u,u} = \frac{\partial^2 C(u,v)}{\partial^2 u}$ *and* $C_{u,v} = \frac{\partial^2 C(u,v)}{\partial u \partial v}$ *are Lipshitz continuous on* $[0,1]^2$. *If* $m = O(n^a)$, *with* $2/5 < a < 3/5$, *then we have*

$$\widehat{CH}_{m,n}(p) - CH(p) = n^{-1} \sum_{i=1}^{n} \nu_i(p) + o_p(n^{-1/2} m^{1/4}),$$

where

$$\nu_i(p) = \mathbb{E}_H \left[H W_{i,m}(F_H(H), p) \right].$$

Theorem 2 can be used to establish the asymptotic normality of the nonparametric estimator of CH with mean zero and - by adapting the proofs in Janssen et al. (2016) - asymptotic variance of order $O(n^{-1} m^{1/2})$. This asymptotic variance, however, is unknown as it depends on C_u. In practice we suggest to use bootstrap for constructing confidence intervals around $\widehat{CH}_{m,n}(p)$.

5 Monte Carlo simulations

In this section, we run Monte Carlo simulations to assess the performance of the estimators of the concentration health that we proposed previously. In particular, we compute the Integrated Mean Square Errors (IMSE) of semiparametric and nonparametric estimators of health concentration curves, which we compare with the IMSE of the classical empirical estimator.

We consider several data-generating processes (DGPs) to model the dependence structure between the health H and the socioeconomic Y variables. We use different copula functions that generate data under different degrees of dependence measured by different values of Kendall's tau coefficient τ. The copulas under consideration are Gaussian copula, Student copula, Clayton copula, and Gumbel copula. The values of Kendall's tau coefficient τ under consideration are: (i) $\tau = (-0.4, 0.001, 0.01, 0.1, 0.2, 0.5, 0.7)$ for Gaussian and Student copulas and (ii) $\tau = (0.001, 0.01, 0.1, 0.2, 0.5, 0.7)$ for Clatyton and Gumbel copulas. Furthermore, to generate the data of the variables of interest H and Y, we use an exponential distribution with the parameter $\lambda = 1$ and a Weibull distribution with the scale and shape parameters $\lambda = 2$ and $k = 10$, respectively.

The performances of the estimators $\widehat{CH}(p)$, $\widehat{CH}_{m,n}(p)$ and $\widehat{CH}_n(p)$ are assessed based on the IMSE that we calculate under different samples sizes: $n = 50$, 100, 200, and 500. Calculation of IMSE is based on $B = 1,000$ Monte Carlo replications. Formally, the IMSE is given by:

$$\text{IMSE} \approx \frac{1}{I} \sum_{i=1}^{I} \left(\frac{1}{B} \sum_{j=1}^{B} \left(\widehat{CH}_j(p_i) - CH(p_i) \right)^2 \right),$$

where $p_i = 0.01, 0.02, \ldots, 0.99$, and $\widehat{CH}_j(p_i)$, for $j = 1, \ldots, B$, is the estimator of the concentration health $CH(p_i)$ that corresponds to the j-th replication. The integral $\int (.)$ of the MSE is approximated by replacing it with the sum $\sum^I (.)$ for $I = 99$.

For the semiparametric estimator $\widehat{CH}(p)$, we assume that the parametric copula is unknown and we use the **BiCopSelect** function implemented in **VineCopula R** package to select the appropriate copula function from a set of copula families. This approach is expected to alleviate the negative effect that the misspecification of the copula model might have on the semiparametric estimator. We recall that copulas can be selected according to Akaike or Bayesian Information Criteria [AIC and BIC, respectively]; see Akaike (1973), Schwarz (1978), and Manner (2007). To do so, all available copulas are first fitted using maximum pseudo-likelihood estimation. Then the information criteria - that are based on the log-likelihood functions - of all fitted copula families are computed, and the copula that has the minimum AIC or BIC is selected. Formally, the AIC of a bivariate parametric copula density $c(F_H(H), F_Y(Y), \theta)$ that depends on parameter vector θ is defined as

$$AIC = -2 \sum_{i}^{n} ln[c(\hat{F}_H(H_i), \hat{F}_Y(Y_i), \hat{\theta}_n) + 2\kappa,$$

where κ represents the number of parameters: e.g.; $\kappa = 1$ for a copula that depends on one parameter, and $\kappa = 2$ for a copula with two parameters. Similarly, the BIC of bivariate copula density $c(F_H(H), F_Y(Y), \theta)$ is given by

$$BIC = -2 \sum_{i}^{n} ln[c(\hat{F}_H(H_i), \hat{F}_Y(Y_i), \hat{\theta}_n) + ln(n)\kappa.$$

Furthermore, the bandwidth parameter m that we use to calculate the nonparametric estimator $\widehat{CH}_{m,n}(p)$ is selected according to the rule of thumb $m = \left[a \times n^{2.5/5}\right]$, where [.] represents the integer part of $a \times n^{2.5/5}$. We consider various values of $m \in \{1, 2, 3, 4, 5\}$ to evaluate the sensitivity with respect to the estimation results. This is a common practice in nonparametric estimation where no optimal bandwidth is available. Using simulations, we find that the optimal value of a that works for all DGPs under consideration corresponds to the value 4, thus to save space we only report results for $a = 4$; see Table 1. The other values of a also provide reasonable results (results for all values of a are available upon request).

The results in Table 1 show that the IMSEs of all estimators are decreasing with the sample size. Interestingly, we find that the semiparametric estimator dominates both the empirical and the nonparametric estimators as it has the smallest IMSE under different copulas, degrees of dependence and sample sizes, except when the dependence between H and Y is weak or when τ takes values between 0.001 and 0.1. Thereafter, we find that the second best estimator corresponds to the nonparametric estimator, which does better than the empirical estimator, except when the degree of dependence between H and Y takes values between $\tau = 0.5$ and $\tau = 0.7$ for some copulas like Gaussian and Gumbel.

The above results correspond to the case where the marginal distributions of H and Y are given by the exponential distribution with parameter $\lambda = 1$. We have obtained additional results after replacing the exponential distribution by the Weibull distribution with the parameters $\lambda = 2$ and $k = 10$. To save space, these results are not reported here, but they are available upon request. Using Weibull as a marginal distribution of H and Y, we find similar results to those discussed previously. The best estimator in terms of IMSE corresponds to the semiparametric estimator $\widehat{CH}(p)$, followed by the Bernstein estimator $\widehat{CH}_{m,n}(p)$ and then the empirical estimator $\widehat{CH}_n(p)$.

6 Inequality in COVID-19's infection and death

Since January 2020, COVID-19 pandemic led to millions of infections and deaths, and caused distressing economic worldwide. Recognizing the importance of many measures - e.g. lockdowns, testing, face masks, and hand-washing - in reducing the transmission of COVID-19, concerns have arisen about the link between pre-existing social and economic inequalities and inequalities in the number of COVID-19's infections and deaths across social classes, with the most-deprived classes are worst hit. In the United States, the spread of COVID-19 across the states have shown that not all Americans are equally at risk of infection and mortality from the virus. In addition, the World Health Organization (WHO) in the European Region pointed out that COVID-19's exposure risk and the severity of its health, social and economic impacts are not being felt equally in the European countries.

Table 1: Integrated Mean Squared Error of Semiparametric ($\widehat{CH}$), Empirical ($\widehat{CH}_n$) and Nonparametric ($\widehat{CH}_{m,n}$) estimators of CH. Simulation results based on 1000 replicates of $10^3 \times$ IMSE of the concentration health estimators.

Copula	τ	$n = 50$			$n = 100$			$n = 200$			$n = 500$		
		$\widehat{CH}$	$\widehat{CH}_n$	$\widehat{CH}_{m,n}$	$\widehat{CH}$	$\widehat{CH}_n$	$\widehat{CH}_{m,n}$	$\widehat{CH}$	$\widehat{CH}_n$	$\widehat{CH}_{m,n}$	$\widehat{CH}$	$\widehat{CH}_n$	$\widehat{CH}_{m,n}$
Gaussian	-0.4	1.52405	2.37677	2.14225	0.81371	1.15701	1.06885	0.38623	0.58638	0.53311	0.12977	0.22836	0.22454
	0.001	2.10629	3.44384	1.88307	1.07944	1.68181	1.00998	0.50564	0.85069	0.49509	0.19713	0.32445	0.19456
	0.01	2.13191	3.38774	1.85736	1.06366	1.73533	0.96506	0.51634	0.82562	0.51147	0.20159	0.32712	0.20469
	0.1	1.79796	3.20303	1.85608	0.87136	1.62803	1.04206	0.41574	0.81374	0.51939	0.17935	0.31983	0.22626
	0.2	1.50939	3.10968	1.86665	0.79499	1.50698	0.97972	0.46025	0.77342	0.51299	0.18221	0.30089	0.25418
	0.5	1.45913	1.98083	2.04345	0.84333	1.06459	1.17494	0.36143	0.51315	0.54520	0.10408	0.19161	0.16909
	0.7	1.08239	1.22984	1.44666	0.64150	0.64480	0.85689	0.22934	0.31696	0.27078	0.08308	0.12031	0.11829
Student	-0.4	1.50998	2.41594	2.09419	0.91477	1.32553	1.14913	0.45419	0.64521	0.57807	0.15306	0.25293	0.23254
	0.001	2.69858	3.84649	2.17324	1.34693	1.89724	1.13122	0.66351	0.98423	0.62257	0.22396	0.40470	0.24812
	0.01	2.79426	3.90271	2.18947	1.37388	1.85705	1.17449	0.68979	1.00119	0.62375	0.21079	0.38427	0.25512
	0.1	2.34374	3.67801	2.05408	1.15942	1.84015	1.14661	0.52027	0.95107	0.60335	0.20992	0.38355	0.26273
	0.2	2.00519	3.63507	2.12335	1.04043	1.70332	1.15646	0.53195	0.86679	0.61781	0.20103	0.34301	0.28498
	0.5	1.41260	2.04994	2.02757	0.74987	1.02980	1.01611	0.36943	0.48307	0.44746	0.15646	0.2214	0.24387
	0.7	1.05205	1.27782	1.44762	0.57896	0.62840	0.75690	0.34523	0.36431	0.48286	0.12641	0.14386	0.21322
Clayton	0.001	2.09081	3.42189	1.87387	1.00368	1.62497	0.91140	0.53735	0.83230	0.50405	0.21267	0.34863	0.20759
	0.01	2.04309	3.39695	1.87465	1.06874	1.62283	1.01943	0.51462	0.84717	0.51277	0.21135	0.34748	0.21627
	0.1	1.95105	3.44810	1.91312	0.91821	1.61878	1.02497	0.38758	0.82406	0.50239	0.13228	0.32879	0.20838
	0.2	1.55803	3.16271	1.76030	0.76749	1.56814	1.00488	0.34245	0.79809	0.49569	0.13989	0.31672	0.21340
	0.5	1.05728	2.33026	1.46983	0.46329	1.13629	0.88551	0.27416	0.55912	0.45783	0.09539	0.24638	0.20293
	0.7	0.84169	1.63300	1.34834	0.42886	0.76142	0.66166	0.20152	0.40266	0.35363	0.07494	0.16145	0.15101
Gumbel	0.001	2.23206	3.52253	1.96451	1.10604	1.72069	1.01641	0.51837	0.83419	0.50979	0.22490	0.36063	0.21245
	0.01	2.17886	3.53497	1.87014	1.02629	1.63997	0.98007	0.54707	0.83069	0.49453	0.21463	0.34587	0.20453
	0.1	2.08629	3.47387	1.99008	1.11354	1.71672	1.15681	0.54978	0.89121	0.60417	0.21383	0.35531	0.27247
	0.2	2.06448	3.18206	2.31921	1.01851	1.53778	1.27509	0.56014	0.81521	0.70188	0.20091	0.30514	0.39143
	0.5	1.35059	1.81019	1.91188	0.77963	0.94400	1.04940	0.37581	0.46746	0.50481	0.13160	0.18465	0.17968
	0.7	1.08024	1.15756	1.47898	0.62124	0.64797	0.85754	0.31388	0.32589	0.40235	0.09029	0.11647	0.11790

Moreover, a growing number of papers have studied how social classes in our societies are affected by Covid-19. These papers examined the impact of socioeconomic variables on COVID-19's infection and death rates, i.e.; impact of variables that make for example low-income communities and people of color more vulnerable than others, see Chen and Krieger (2021), Chin et al. (2020), McLaren (2021), and Brown and Ravallion (2020). However, none of the above-mentioned studies use proper measures of health that are designed to detect inequalities in rates of COVID-19's infections and deaths across socio-economic covariates. These studies are based on simple correlations and regressions and might not help detect inequalities in COVID-19's infections and deaths. In this section, we use our previously developed semi/nonparametric estimators of CH to quantify and examine inequalities in COVID-19's infections and deaths across and within the U.S. states. The next subsection discusses the U.S. data we use for our empirical analysis. Our results show that effectively socio-economic variables like poverty, race, and economic prosperity of a state might explain inequalities in COVID-19's infections and deaths.

6.1 Data

We begin by describing our data and provide some descriptive statistics. Micro-data on COVID-19's cases and deaths that include socio-economic characteristics at unit-record level (county level for the U.S. data) are less frequent. To obtain our data, we had to merge recorded counts of cases and deaths in the U.S. at county level with socio-economic characteristics-average incomes, race, income inequality and poverty. Our dataset contains information about 2777 counties across 45 U.S. states. We excluded five U.S. states because of insufficient data, i.e.; in each of these states we have very few counties and this is not enough for the estimation of health concentration curves. These states are: Kansas, Kentucky, Louisiana, Maine, Nevada. Our county-level variables fall into three general categories:

- Health variables on confirmed COVID-19's cases and deaths.
- Socio-economic variables on the percentage of population below the poverty line, percentage of residents that are African American, percentage of White people, percentage of Asian, median income, and total population.
- Inequality variables such as Gini (economic) index and Gini health index that we estimate using the semiparametric estimator in (11).

For data on confirmed COVID-19's cases and deaths, we draw on the U.S. Centers for Disease Control and Protection (CDC).[2] We use the most recent numbers available at the time of writing this paper (June 10, 2021). Data on county's population, population density, demographics and poverty rates were obtained from the US Census Bureau. Median income, and the poverty rate are estimated from survey data, but complemented by small-area estimation methods [see Rao and Molina (2015)]. Descriptive statistics of COVID-19's infection and death rates and socio-economic variables in the 2777 counties can be found in Table 2. In this table, the share of Black Americans refers to the proportion of the population that identifies as Black only, while the share "White" refers to the proportion of the population that identifies as White. The table shows that the average number of infections and deaths per county are 9.8% and 1.9%, while their standard deviation are 2.99% and 1%, respectively. Crowley county in Colorado recorded the highest number of cases (37%) and the second highest percentage of cases are in Chattahoochee in Georgia (36.8%). We also find that, overall, the average of poverty rate is 14.3%, ranging from 2.3% in Sterling County (Texas) to 54.7% in Todd County (South Dakota). Gini (economic) index is also estimated using small-area methods and varies widely across counties, from the lowest value of 0.302 in Skagway County (Alaska) to the highest value of 0.609 in Harding County (New Mexico). Furthermore, in Table 3 we report the correlation coefficients matrix of the socio-economic variables that we use in our empirical analysis. From this, we find a significant positive correlation between share of Black Americans and poverty rate and a significant but negative correlation between share of White Americans and poverty rate. We next provide the results of the estimation of health concentration curves using the above data.

6.2 Estimation of health concentration curve

As we mentioned earlier, the health concentration curve $CH(p)$ allows one to obtain plots of cumulative percentage of the health variable - here COVID-19's infection and death rates - against the cumulative percentage of the population ranked by the socio-economic covariate - here poverty rate, population density, share of Black Americans, share of White Americans, etc. These plots help visualize health inequalities by observing the position of the health concentration curve with respect to the line of equality (45-degree line) in a two-dimensional space. When the higher the socio-economic variable is the richer the individual is, if $CH(p)$ lies above the 45-degree line, then health inequality is referred

[2] The data are available through USA Facts : https://usafacts.org/visualizations/coronavirus-covid-19-spread-map/. An alternative source is the New York Times data site for COVID-19 (obtainable from the their Github repository). The NYT site, however, records cases and deaths according to the county in which they occurred, while CDC does so according to the person's place of residence.

Table 2: Summary statistics

	Mean	**Std Dev.**	**Min**	**Max**
Cases	0.098	0.0299	0.0029	0.375
Deaths	0.019	0.010	0.000	0.102
Population	106542	341079	66	10081570
Population density	214.77	778.96	0.000	17179
Poverty rate	0.143	0.058	0.023	0.547
Median income	27776	5850	8641	70390
Gini Index	0.444	0.035	0.302	0.609
Share of Black Americans	0.089	0.144	0	0.872
Share of White Americans	0.756	0.203	0.006	1
Share of Asian Americans	0.013	0.028	0	0.417

Note: This table provides the descriptive statistics of COVID-19's infection and death rates and socio-economic variables for 2777 counties of 45 U.S. states. Data on COVID-19's cases and deaths rates are obtained from U.S. Centers for Disease Control and Protection (CC) and covers the period until June 10, 2021. Demographic variables are drawn primarily from the US Census and CDC.

Table 3: Correlation coefficients between socio-economic variables

	Density	**Median income**	**Population**	**Poverty rate**
Median income	0.296			
Population	0.366	0.227		
Poverty rate	-0.052	-0.742	-0.076	
Share of Black Americans	0.128	-0.263	0.057	0.441
Share of White Americans	-0.185	0.194	-0.224	-0.475

Note: The table shows the correlation coefficients matrix of socio-economic variables we use in our empirical analysis. These variables are described in Table 2.

to as pro-rich - i.e., the rich have better health than the poor -, and in this case the associated health concentration index is negative. When $CH(p)$ lies under the 45-degree line, the health inequality is considered pro-poor - i.e., the poor have better health than the rich-, and the associated health concentration index is positive. If the health concentration curve coincides with the 45-degree line, then there is no socioeconomic health inequality, and the associated health concentration index is necessarily zero.

We now use the data described in the previous subsection to calculate the semiparametric and nonparametric estimators of health concentration curve for COVID-19's infection and death rates. For each state, we use three socioeconomic variables: income, poverty, and proportion of white/black people. We got the results for all 45 U.S. states, but for a better presentation we only report the results for average, low and high income states, average, low and high poverty rate states, and average, low and high share of white people states [rest of the results are available upon request]. The results are reported in Figures 3 to 11 of the appendix. Using income as a socio-economic variable, Figures 3 and 4 show a clear pro-rich inequality for COVID-19's death rate both in low and high income states, except for West Virginia. Interestingly, for the average income states [see Figure 5], we find that the health concentration curve tend to match the 45-degree line, which indicates that individuals in these states had equal chance of dying from COVID-19 regardless of their socioeconomic position. We reach similar results when we replace income by poverty rate noting that low poverty rate is expected to be highly correlated with high income and vice-versa. Figures 6 and 7 confirm the pro-rich inequality for COVID-19's death rate for both low and high poverty rate states, with health concentration curve lies below the 45-degree line when the higher the poverty rate is the poorer the county is. The result in Figure 8 is also similar to the one we obtained in Figure 5: there is no inequality in COVID-19's death rate in the states with average poverty rate as the health concentration curve matches the 45-degree line. Moreover, Figures 9 and 10 indicate that the inequality in COVID-19's death rate is generally in favor of counties with low share of white people, except in state of California. However, the opposite happens in states with average share of white people, where we see that the inequality in COVID-19's death rate is in favor of counties with high share of white people.

To sum up, it seems that the socio-economic variables income, poverty rate and ethnicity have an impact on COVID-19's death rate, with the most-deprived classes are worst hit by the virus. In the next subsection, we provide further analysis using econometric models that link COVID-19's cases and deaths to the Gini health index and other key socio-economic covariates.

Table 4: Regressions for COVID1-19 deaths

	Dependent variable: Log(COVID-19's deaths)						
	(1)	**(2)**	**(3)**	**(4)**	**(5)**	**(6)**	**(7)**
Constant	7.87*** (0.17)	6.63*** (0.60)	−6.61** (3.46)	−7.47** (3.57)	−3.82 (3.60)	−6.64** (3.61)	−7.52** (3.70)
Population	0.13*** (0.01)	0.12*** (0.01)	0.08*** (0.017)	0.08*** (0.01)	0.09*** (0.01)	0.09*** (0.01)	0.09*** (0.015)
Poverty rate		10.19** (4.79)	0.93 (4.79)	0.037 (4.87)	−0.872 (4.69)	−7.78 (4.89)	
Gini index			31.6** (8.18)	33.5*** (8.39)	20.54*** (8.42)	30.36*** (8.53)	29.8*** (7.57)
Gini health index				1.68 (1.68)		4.00** (1.92)	3.87** (1.85)
Share of Black Americans					2.76** (1.34)	1.57 (1.34)	1.41 (1.33)
Share of Asian Americans						−6.91*** (2.31)	−7.24*** (2.31)
Median income							5.36** (2.94)

Note: This table reports the estimation results of regressing state-level COVID-19's death on state's population size, state's poverty rate, state's median income, state's Gini (economic) index, state's Gini health index, state's share of Black Americans, and state's share of Asian Americans,. The dependent variable is log (COVID-19's deaths). Standard errors in parentheses. *p<0.1; **p<0.05; ***p<0.01.

6.3 Further analysis

In this subsection, we use U.S. state-level data and regression models for further analysis on the impact of social and health inequalities on COVID-19's infections and deaths. We regress state-level COVID-19's infections and deaths on measures of health and economic inequalities and key socio-economic variables. In our regressions, we include all or some of the following variables: state's population size, state's poverty rate, state's median income, state's Gini (economic) index, state's Gini health index, state's share of Black Americans, and state's share of Asian Americans. The results are reported in Tables 4-5.

The results in Tables 4-5 show that both economic (Gini index) and health (Gini health index) inequality measures have a positive impact on COVID-19's infections and deaths after controlling for key socio-economic variables. These effects are generally statistically significant. The effects of poverty rate on COVID-19's infections and deaths are statistically insignificant, which might be explained by the fact that we control for other variables that are highly correlated with the poverty rate. In addition, the median income and population size have significant and positive impacts on

Table 5: Regressions for COVID1-19 infections

	Dependent variable: log(COVID-19's cases)						
	(1)	**(2)**	**(3)**	**(4)**	**(5)**	**(6)**	**(7)**
Constant	12.1^{***} (0.14)	11.3^{***} (0.50)	4.62 (3.17)	3.69 (3.25)	7.09^{**} (3.30)	3.75 (3.08)	3.39 (3.22)
Population	0.11^{***} (0.01)	0.11^{***} (0.01)	0.09^{***} (0.01)	0.09^{***} (0.01)	0.09^{***} (0.015)	0.10^{***} (0.01)	0.10^{***} (0.01)
poverty rate		6.35 (3.95)	1.66 (4.38)	0.69 (4.44)	0.05 (4.31)	−7.84 (4.19)	
Gini index			16.0^{**} (7.48)	18.0^{**} (7.64)	10.5 (7.72)	20.1^{***} (7.30)	15.8^{**} (6.58)
Gini health index				1.82 (1.53)		4.73^{***} (1.64)	4.42^{***} (1.61)
Share of Black Americans					2.45^{**} (1.23)	1.05 (1.14)	0.92 (1.15)
Share of Asian Americans						-7.84^{***} (1.97)	-7.79^{***} (2.01)
Median income							4.41^{**} (2.55)

Note: This table reports the estimation results of regressing state-level COVID-19's infections (cases) on state's population size, state's poverty rate, state's median income, state's Gini (economic) index, state's Gini health index, state's share of Black Americans, and state's share of Asian Americans. The dependent variable is log (COVID-19's cases). Standard errors in parentheses. *p<0.1; **p<0.05; ***p<0.01.

both COVID-19's infections and deaths, whereas the impact of share of Black Americans is positive and generally statistically insignificant and the impact of the share of Asian Americans is negative and statistically significant. The results we obtained for COVID-19's infections and deaths are very similar.

The above results confirm once again that greater economic and health inequalities led to higher COVID-19's infection and death rates, with the most-deprived classes are worst hit. Thus, policy-makers are urged to set containment measures to reduce COVID-19's infections and deaths among most-deprived classes. At short-term, measures like free masks and sanitizers and targeted vaccination campaigns should help reduce COVID-19's infection and death rates in deprived states. At long-term, governments should set measures that can help reduce economic and social inequalities in society, which in turn will reduce health inequality.

7 Conclusion

We derived semi/non-parametric estimators of Health Concentration curve (HC) that can quantify inequalities in COVID-19 infections and deaths and help identify the social classes that are most at risk of infection and dying from the virus. We expressed HC in terms of copula function that we used to build our estimators of HC. For the semi-parametric estimator, a parametric copula was used to model the dependence between health and socio-economic variables. The parameters of the copula were estimated using maximum pseudo-likelihood estimator after replacing the cumulative distribution of health variable by its empirical analogue. For the non-parametric estimator, we replaced the copula function by the Bernstein copula estimator. Furthermore, we used the estimators of HC to derive semi/non-parametric estimators of health Gini coefficient. We establish the consistency and asymptotic normality of the estimators of HC. Using different data-generating processes and sample sizes, a Monte-Carlo simulation exercise showed that the semiparametric estimator outperforms the Bernstein-copula-based estimator, and that the latter does better than the empirical estimator in terms of Integrated Mean Squared Error. We also run an extensive empirical study to illustrate the importance of HC estimators for investigating inequality in COVID-19 infections and deaths in the U.S. The empirical results showed that socio-economic variables like poverty, race, and economic prosperity of a state can explain the observed inequalities in COVID-19 infections and deaths.

References

[1] Akaike, H. (1998). “Information theory and an extension of the maximum likelihood principle,” In Selected papers of hirotugu akaike, Springer, New York, NY, pp. 199-213.

[2] Allison, R. A. and Foster, J. E. (2004). “Measuring health inequality using qualitative data,” *Journal of Health Economics,* vol. 23 (3), pp. 505-524.

[3] Bermudi, P. M. M., Lorenz, C., de Aguiar, B. S., Failla, M. A., Barrozo, L. V., & Chiaravalloti-Neto, F. (2021). “Spatiotemporal ecological study of COVID-19 mortality in the city of São Paulo, Brazil: shifting of the high mortality risk from areas with the best to those with the worst socio-economic conditions,” *Travel medicine and infectious disease*, vol. 39, 101945.

[4] Bouezmarni, T., Rombouts, J., and Taamouti, A. (2010). “Asymptotic properties of the Bernstein density copula estimator for -mixing data,” *Journal of Multivariate Analysis*, vol. 101, pp. 1-10.

[5] Brown, C. S., and Ravallion, M. (2020). “Inequality and the coronavirus: Socioeconomic covariates of behavioral responses and viral outcomes across US counties,” (No. w27549). National Bureau of Economic Research.

[6] Chen, J. T., and Krieger, N. (2021). “Revealing the unequal burden of COVID-19 by income, race/ethnicity, and household crowding: US county versus zip code analyses,” *Journal of Public Health Management and Practice*, vol. 27(1), pp. S43-S56.

[7] Chin, T., Kahn, R., Li, R., Chen, J.T., Krieger, N., Buckee, C.O., Balsari, S., and Kiang, M.V. (2020). “U.S. county-level characteristics to inform equitable COVID-19 response,” medRxiv preprint.

[8] Deheuvels, P. (1979). “La fonction de dépendance empirique et ses propriétés. Un test non paramétrique d’indépendance,” *Bulletins de l’Académie Royale de Belgique*, vol. 65(1), pp. 274-292.

[9] Ehlert, A. (2021). “The socio-economic determinants of COVID-19: a spatial analysis of German county level data,” *Socio-Economic Planning Sciences*, 101083.

[10] Erreygers, G. and Van Ourti, T. (2011). “Measuring socioeconomic inequality in health, health care and health nancing by means of rank-dependent indices: a recipe for good practice,” *Journal of Health Economics*, vol. 30(4), pp. 685-694.

[11] Genest, C., Ghoudi, K., and Rivest, L. P. (1995). "A semiparametric estimation procedure of dependence parameters in multivariate families of distributions," *Biometrika,* vol. 82(3), pp. 543-552.

[12] Janssen, P., Swanepoel, J., and Veraverbeke, N. (2012). "Large sample behavior of the Bernstein copula estimator," *Journal of Statistical Planing and Inference.* vol. 142, pp. 1189-1197.

[13] Janssen, P., Swanepoel, J., and Veraverbeke, N. (2016). "Bernstein estimation for a copula derivative with application to conditional distribution and regression functionals," TEST vol. 25 (2), pp. 351-374.

[14] Knittel, C. R., and Ozaltun, B. (2020). "What does and does not correlate with COVID-19 death rates," (No. w27391). National Bureau of Economic Research.

[15] Krieger N, Chen, J.T, Waterman, P.D, Rehkopf, D.H, Subramanian, S.V. (2005). "Painting a truer picture of US socioeconomic and racial/ethnic health inequalities: The Public Health Disparities Geocoding Project," Am J Public Health, vol. 95: pp. 312-323.

[16] Krieger N, Chen, J.T, Waterman, P.D, Rehkopf, D.H, Subramanian, S.V. (2003). "Race/ethnicity, gender, and monitoring socioeconomic gradients in health: a comparison of area-based socioeconomic measures-the Public Health Disparities Geocoding Project," *American Journal of Public Health*, vol. 93, pp. 1655-1671.

[17] Krieger N, Chen J.T, Waterman P.D, Soobader M-J, Subramanian, S.V, Carson R. (2002). "Geocoding and Monitoring US Socioeconomic Inequalities in Mortality and Cancer Incidence: Does Choice of Area-Based Measure and Geographic Level Matter?-The Public Health Disparities Geocoding Project," *American Journal of Epidemiology*, vol. 156(5), pp. 471-82.

[18] Krieger N, Chen, J.T, Waterman, P.D, Soobader, M-J, Subramanian, S.V, Carson, R. (2003a). "Monitoring socioeconomic inequalities in sexually transmitted infections, tuberculosis, and violence: Geocoding and choice of area-based socioeconomic measures-The Public Health Disparities Geocoding Project (US)," *Public Health Reports*, vol. 118, pp. 240-260.

[19] Krieger N, Chen, J.T, Waterman, P.D, Soobader, M-J, Subramanian, S.V, Carson, R. (2003b). "Choosing area-based socioeconomic measures to monitor social inequalities in low birthweight and childhood lead poisoning –The Public Health Disparities Geocoding Project (US)," J*ournal of Epidemiology & Community Health*, vol. 57(3), pp. 186-199.

[20] Lassale, C., Gaye, B., Hamer, M., Gale, C. R., and Batty, G. D. (2020). "Ethnic disparities in hospitalisation for COVID-19 in England: The role of socioeconomic factors, mental health, and inflammatory and pro-inflammatory factors in a community-based cohort study," *Brain, behavior, and immunity*, vol. 88, pp. 44-49.

[21] Manner, H. (2007). "Estimation and model selection of copulas with an application to exchange rates," METEOR, Maastricht research school of Economics of Technology and Organizations.

[22] McLaren, J. (2021). "Racial disparity in COVID-19 deaths: Seeking economic roots with census data," *The BE Journal of Economic Analysis & Policy*, vol. 21(3), pp. 897-919

[23] Rao, J. N., & Molina, I. (2015). Small area estimation. John Wiley & Sons.

[24] Shih, J. H., and Louis, T. A. (1995). "Inferences on the association parameter in copula models for bivariate survival data," *Biometrics*, pp. 1384-1399.

[25] Sancetta, A. and Satchell, S. (2004). "The Bernstein copula and its applications to modeling and approximations of multivariate distributions," *Econometric Theory,* vol. 20, pp. 535-562.

[26] Schwarz, G. (1978). "Estimating the dimension of a model," *The Annals of Statistics*, PP. 461-464.

[27] Tsukahara, H. (2005). "Semiparametric estimation in copula models," *Canadian Journal of Statistics*, vol. 33(3), pp. 357-375.

[28] Wagstaff , A. (2002). "Inequality aversion, health inequalities and health achievement," *Journal of Health Economics,* vol. 21, pp. 627-641.

[29] Wagstaff, A. (2005). "The bounds of the concentration index when the variable of interest is binary, with an application to immunization inequality," *Health Economics*, vol. 14 (4), pp. 429-432.

[30] Wagstaff, A., Paci, P., and Van Doorslaer, E. (1991). "On the measurement of inequalities in health," *Social Science & Medicine* vol. 33 (5), pp. 545-557.

[31] Wagstaff, A., Van Doorslaer, E., and Paci, P. (1989). "Equity in the finance and delivery of health care: some tentative cross-country comparisons," *Oxford review of economic policy*, vol. 5(1), pp. 89-112.

[32] Wu, X., Nethery, R. C., Sabath, M. B., Braun, D., and Dominici, F. (2020). "Exposure to air pollution and COVID-19 mortality in the United States," medRxiv, 2020.04.05.20054502.

[33] Zheng, B. (2011). "A new approach to measure socioeconomic inequality in health," *The Journal of Economic Inequality,* vol. 9 (4), pp. 555-577.

8 Appendix: Proofs

This appendix contains the proofs of the main results in the text.

Poof of Proposition 1: Observe that

$$\begin{aligned} CH(p) &= \frac{\int_0^p \mathbb{E}\left[H \mid Y = F^{-1}(u)\right] du}{\int_0^1 \mathbb{E}\left[H \mid Y = F_Y^{-1}(u)\right] du} \\ &= \frac{\int_0^p \int_0^{+\infty} h f_H(h) c(F_H(h), u) dh du}{\int_0^1 \int_0^{+\infty} h f_H(h) c(F_H(h), u) dh du} \\ &= \frac{\int_0^{+\infty} h f_H(h) C_u(F_H(h), p) dh}{\int_0^{+\infty} h f_H(h) C_u(F_H(h), 1) dh} \\ &= \frac{\int_0^1 F_H^{-1}(u) C_u(u, p) du}{\mathbb{E}(H)}, \end{aligned}$$

where the last equality is due to the fact that $\int_0^{+\infty} h f_H(h) C_u(F_H(h), 1) dh = \int_0^{+\infty} h f_H(h) dh = \mathbb{E}(H)$ since $C_u(u, 1) = 1$.

Poof of Theorem 1: We start with the following decomposition

$$\widehat{CH}(p) - CH(p) = \frac{\hat{m}(p) - \bar{H} CH(p)}{\mathbb{E}(H)} + \frac{(\mathbb{E}(H) - \bar{H})(\hat{m}(p) - \bar{H}\, CH(p))}{\mathbb{E}(H)\bar{H}}, \tag{13}$$

where $\bar{H}$ is the empirical mean of H and $\hat{m}(p) = n^{-1}\sum_{i=1}^n H_i C_u(\widehat{F}_H(H_i), p, \widehat{\theta}_n)$. We study the first term in (13) since the second term is negligible with respect to the first term. Using Taylor expansion of C_u around $(F_H(H_i), p, \theta_0)$, we obtain

$$\hat{m}(p) = n^{-1} \sum_{i=1}^n H_i\, C_u(F_H(H_i), p, \theta_0) + I_{n,1} + I_{n,2}, \tag{14}$$

where

$$I_{n,1} = n^{-1} \sum_{i=1}^n H_i\, C_{uu}(\tilde{F}_H(H_i), p, \tilde{\theta})(\widehat{F}_H(H_i) - F_H(H_i))$$

and

$$I_{n,2} = n^{-1} \sum_{i=1}^n H_i\, (\hat{\theta}_n - \theta_0)^\top C_{u,\theta}(\tilde{F}_H(H_i), p, \tilde{\theta}),$$

with

$$\tilde{F}_H(H_i) = F_H(H_i) + \alpha(\widehat{F}_H(H_i) - F_H(H_i)),\ \tilde{\theta} = \theta_0 + \alpha(\hat{\theta}_n - \theta_0),\ \alpha \in (0, 1).$$

Under Assumptions B1 and B2, we have:

$$I_{n,1} = n^{-1} \sum_{i=1}^n H_i\, C_{uu}(F_H(H_i), p, \theta_0)(\widehat{F}_H(H_i) - F_H(H_i)) + o_p(n^{-1/2}),$$

and, from Assumption B4, we obtain

$$\begin{aligned}
I_{n,2} &= n^{-1}\sum_{i=1}^{n} H_i\,(\hat{\theta}_n-\theta_0)^\top C_{u,\theta}(F_H(H_i),p,\theta_0)+o_p(n^{-1/2})\\
&= (\hat{\theta}_n-\theta_0)^\top n^{-1}\sum_{i=1}^{n} H_i\,C_{u,\theta}(F_H(H_i),p,\theta_0)+o_p(n^{-1/2})\\
&= (\hat{\theta}_n-\theta_0)^\top \mathbb{E}\left[H\,C_{u,\theta}(F_H(H),p,\theta_0)\right]+o_p(n^{-1/2})\\
&= \xi_i^\top r_\theta(p,\theta_0)+o_p(n^{-1/2}), \qquad (15)
\end{aligned}$$

where, $r_\theta(p,\theta_0)=\mathbb{E}\left[H\,C_{u,\theta}(F_H(H),p,\theta_0)\right].$

Now, observe that $I_{1,n}$ is a V-statistic with the kernel $h_1(u,v,\theta_0)=\frac{1}{2}\left[h_2(u,v,\theta_0)+h_2(v,u,\theta_0)\right],$ where

$$h_2(u,v,\theta_0)=uC_{uu}(F_H(u),p,\theta_0)(\mathbb{I}(v\le u)-F_H(u)).$$

It can be shown that $\mathbb{E}(h_1(H_i,H_j,\theta_0))=0$, and from Assumption B3, we have $\mathbb{E}(h_1^2(H_i,H_j,\theta_0))<\infty$.

Hence, we obtain

$$I_{n,1}=n^{-1}\sum_{i=1}^{n}\eta(H_i,p,\theta_0)+o_p(n^{-1/2}), \qquad (16)$$

where

$$\eta(H_i,p,\theta_0)=E_H\left[H\left(\mathbb{I}(H_i\le H)-F_H(H)\right)C_{uu}(F_H(H),p,\theta_0)\right].$$

From (14), (15), and (16), we conclude the proof of Theorem 1.

Poof of Theorem 2: From Janssen et al. (2016), and using the conditions of the theorem, we have

$$\widetilde{C}_u(\widehat{F}_H(h),p)=\frac{1}{n}\sum_{i=1}^{n}W_{i,m}(F_H(h),p)+o_p(n^{-1/2}m^{1/4}).$$

Hence,

$$\begin{aligned}
\frac{1}{n}\sum_{j=1}^{n}H_j\widetilde{C}_u(\widehat{F}_H(H_j),p) &= \frac{1}{n}\sum_{j=1}^{n}\left[H_j\frac{1}{n}\sum_{i=1}^{n}W_{i,m}(F_H(H_j),p)\right]+o_p(n^{-1/2}m^{1/4})\\
&= \frac{1}{n}\sum_{i=1}^{n}\left[\frac{1}{n}\sum_{j=1}^{n}H_jW_{i,m}(F_H(H_j),p)\right]+o_p(n^{-1/2}m^{1/4})\\
&= \frac{1}{n}\sum_{i=1}^{n}\mathbb{E}_H\left[HW_{i,m}(F_H(H),p)\right]+o_p(n^{-1/2}m^{1/4}).
\end{aligned}$$

9 Appendix: Empirical results

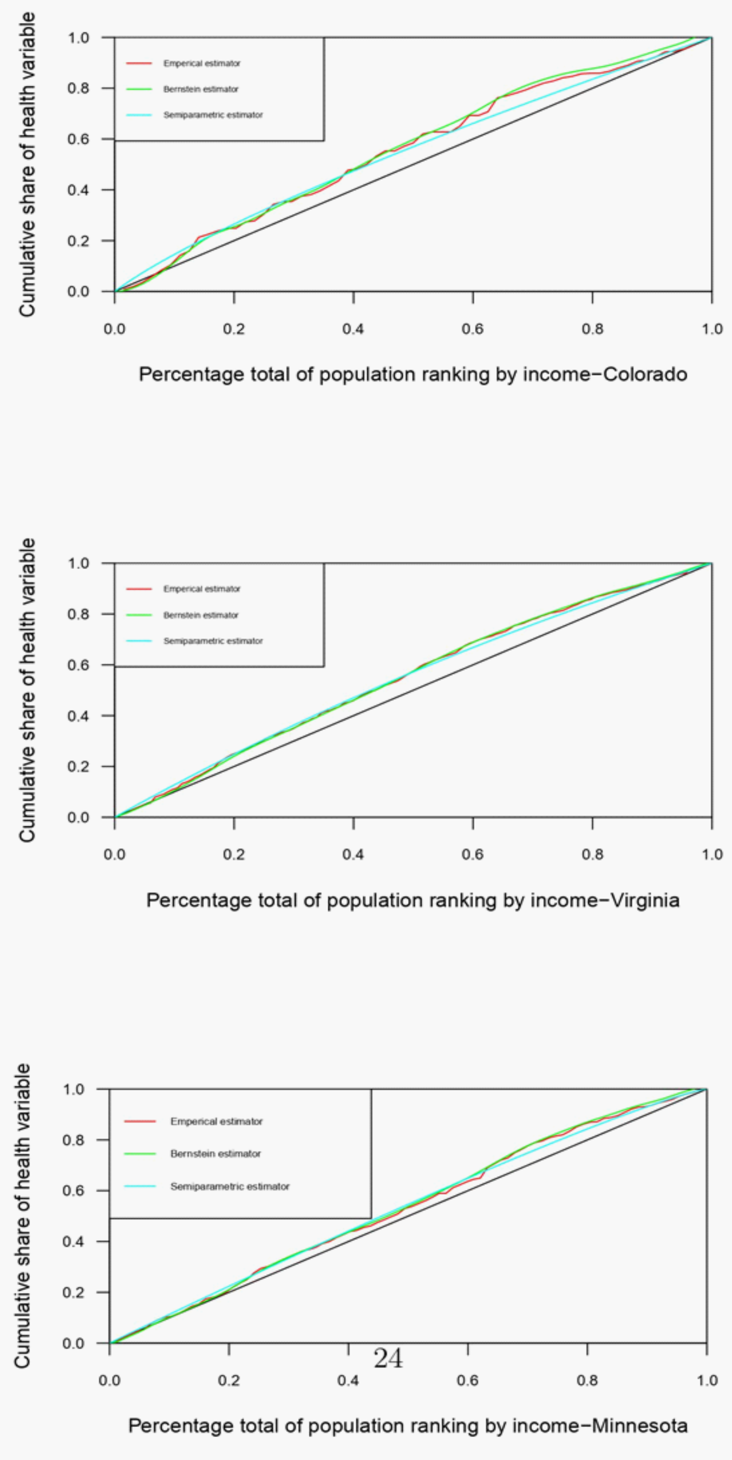

Figure 3: The empirical estimator, the semiparametric and the nonparametric estimator of the health concentration curve for COVID-19deaths. (high income states).

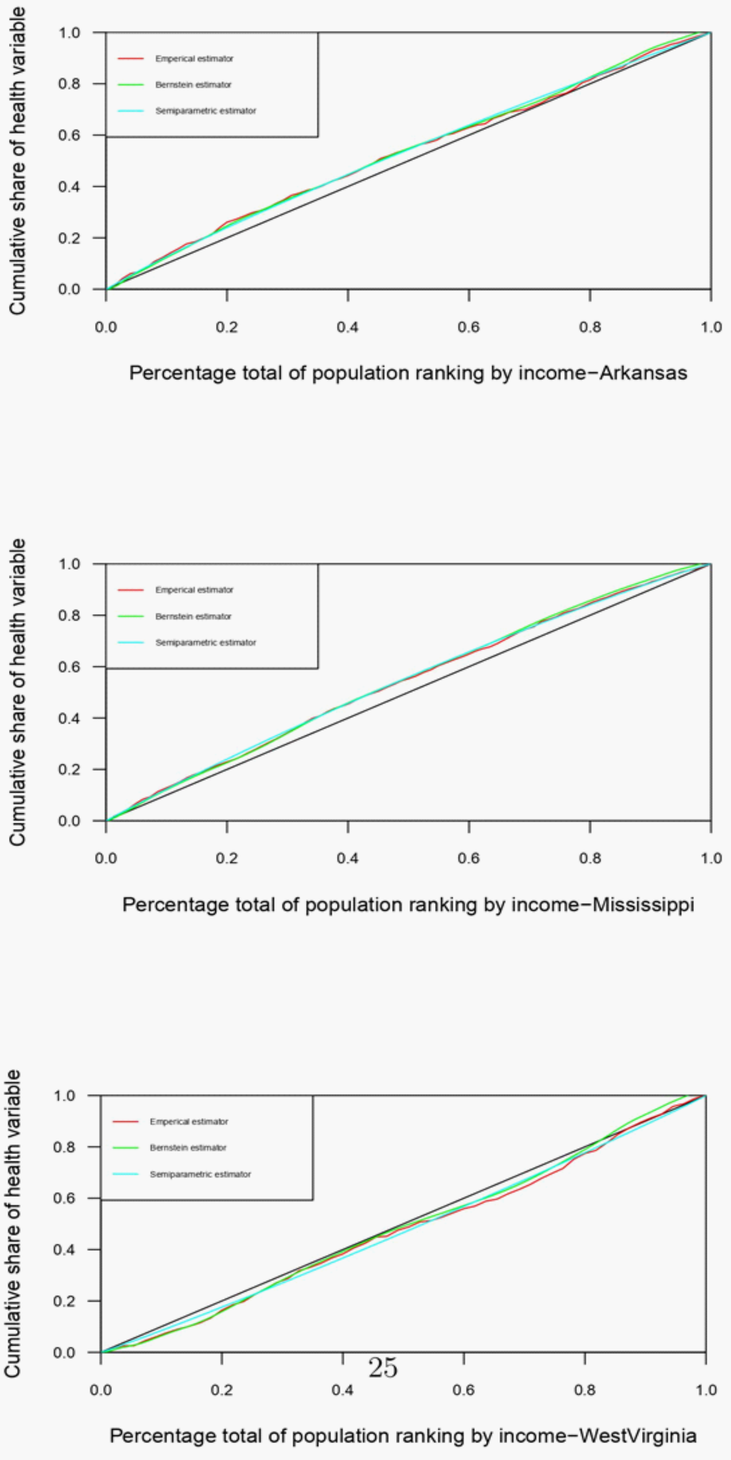

Figure 4: The empirical estimator, the semiparametric and the nonparametric estimator of the health concentration curve for COVID-19deaths. (low income states).

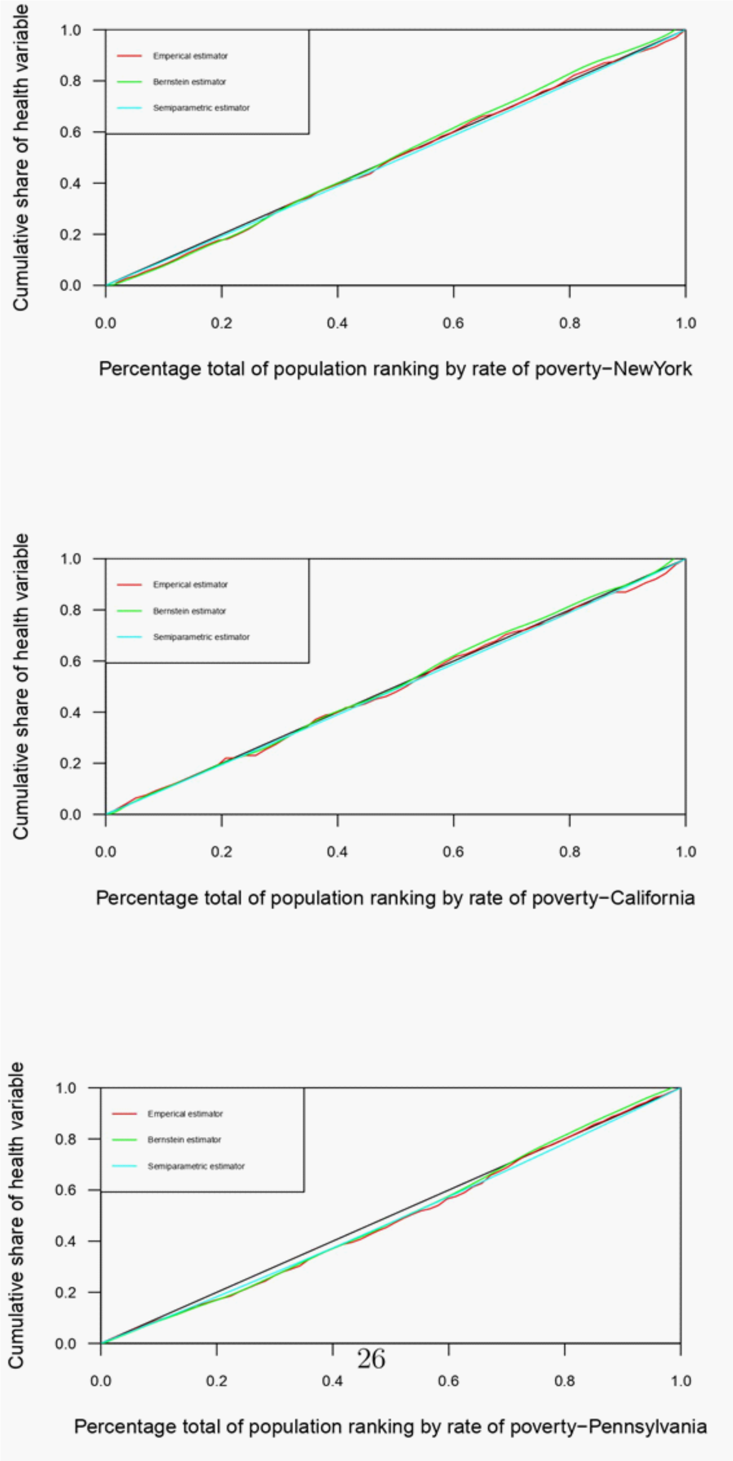

Figure 5: The empirical estimator, the semiparametric and the nonparametric estimator of the health concentration curve for COVID-19deaths. (average income states)

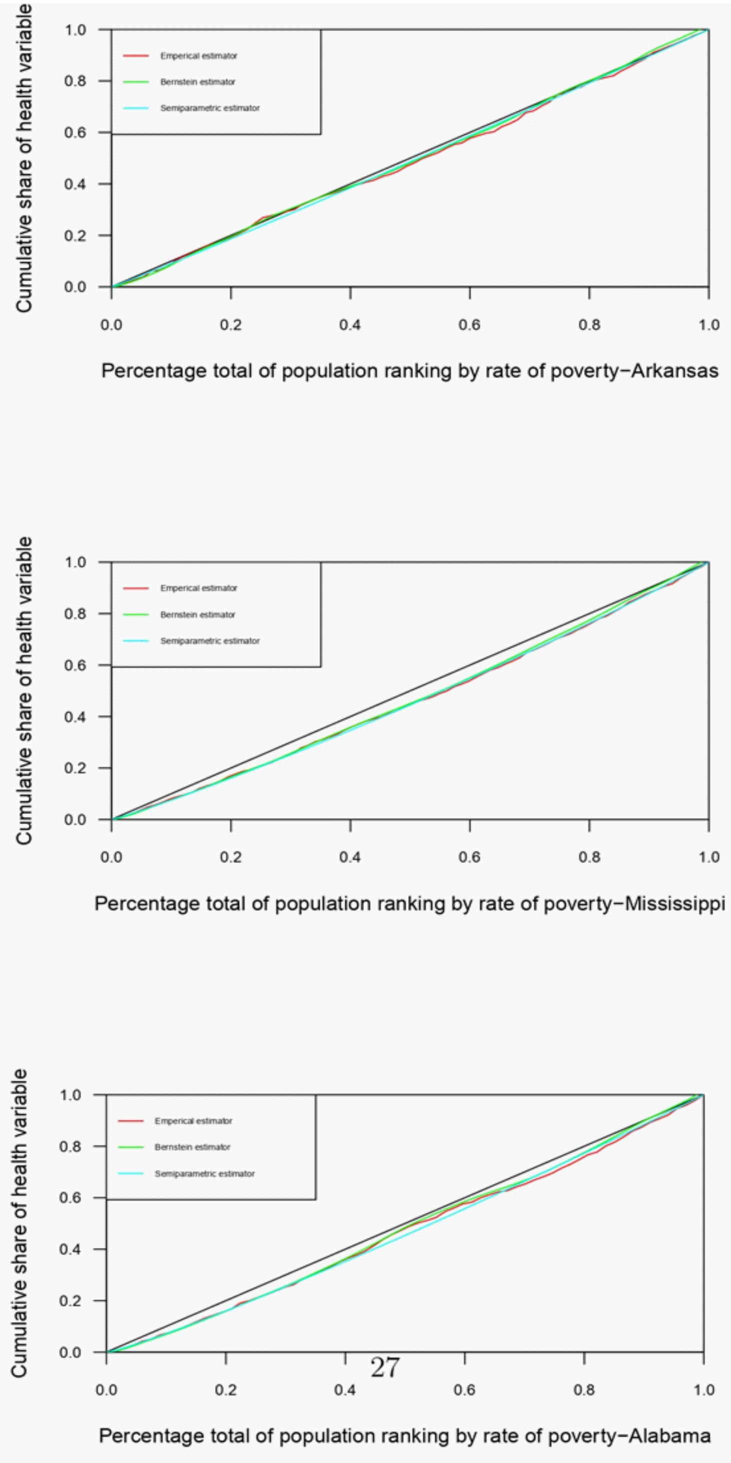

Figure 6: The empirical estimator, the semiparametric and the nonparametric estimator of the health concentration curve for COVID-19deaths. (high poverty rate states).

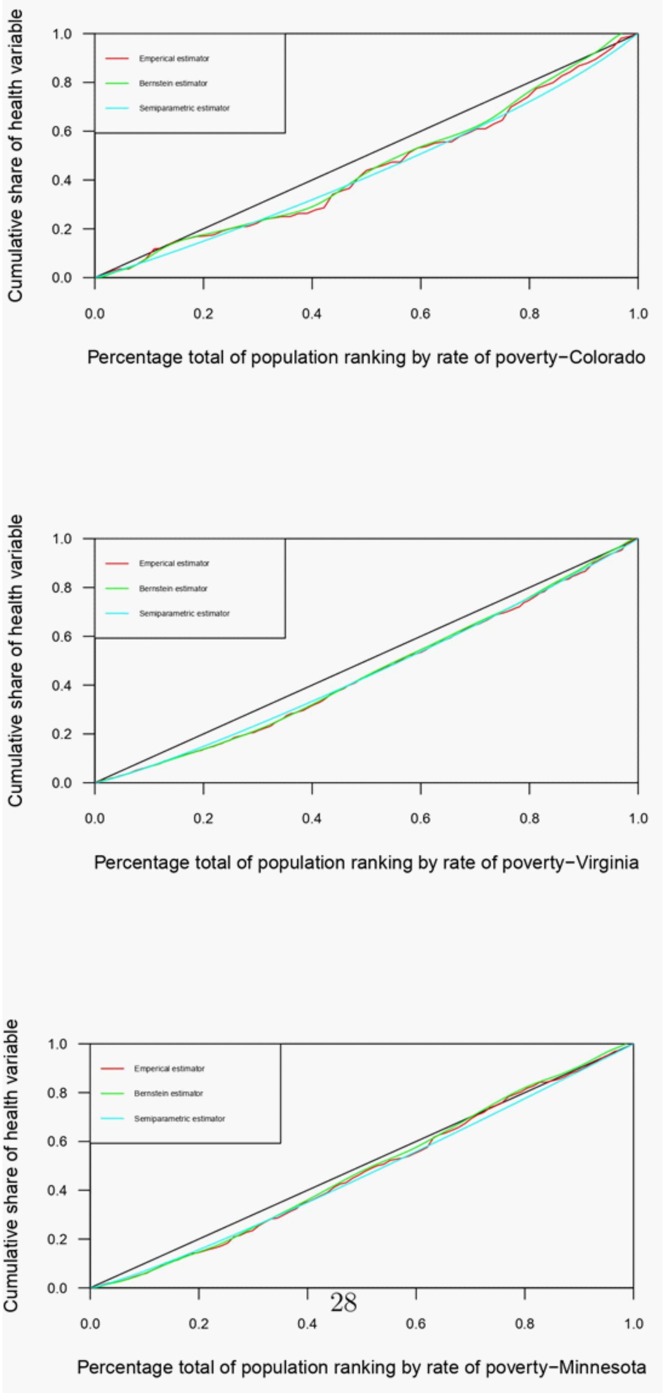

Figure 7: The empirical estimator, the semiparametric and the nonparametric estimator of the health concentration curve for COVID-19deaths. (low poverty rate states).

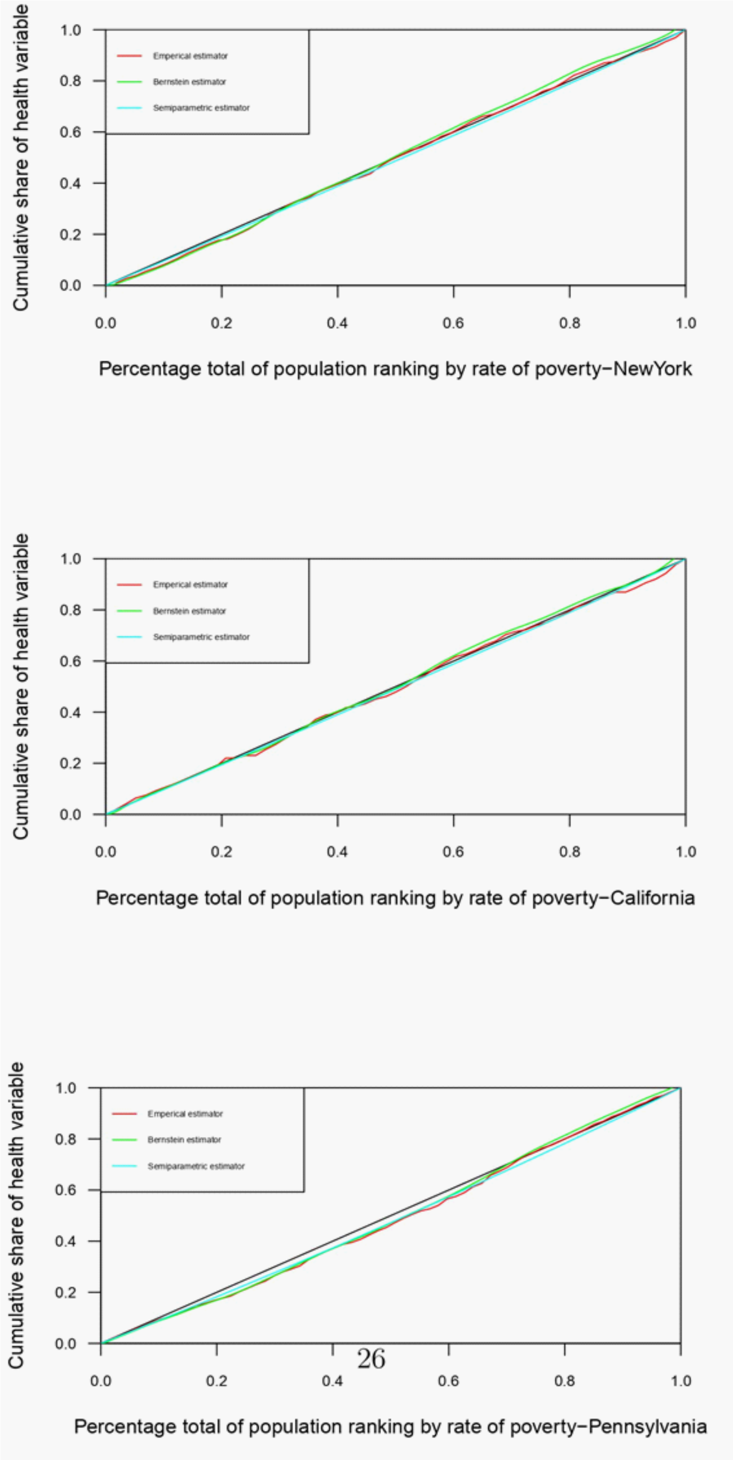

Figure 8: The empirical estimator, the semiparametric and the nonparametric estimator of the health concentration curve for COVID-19deaths. (average poverty rate states).

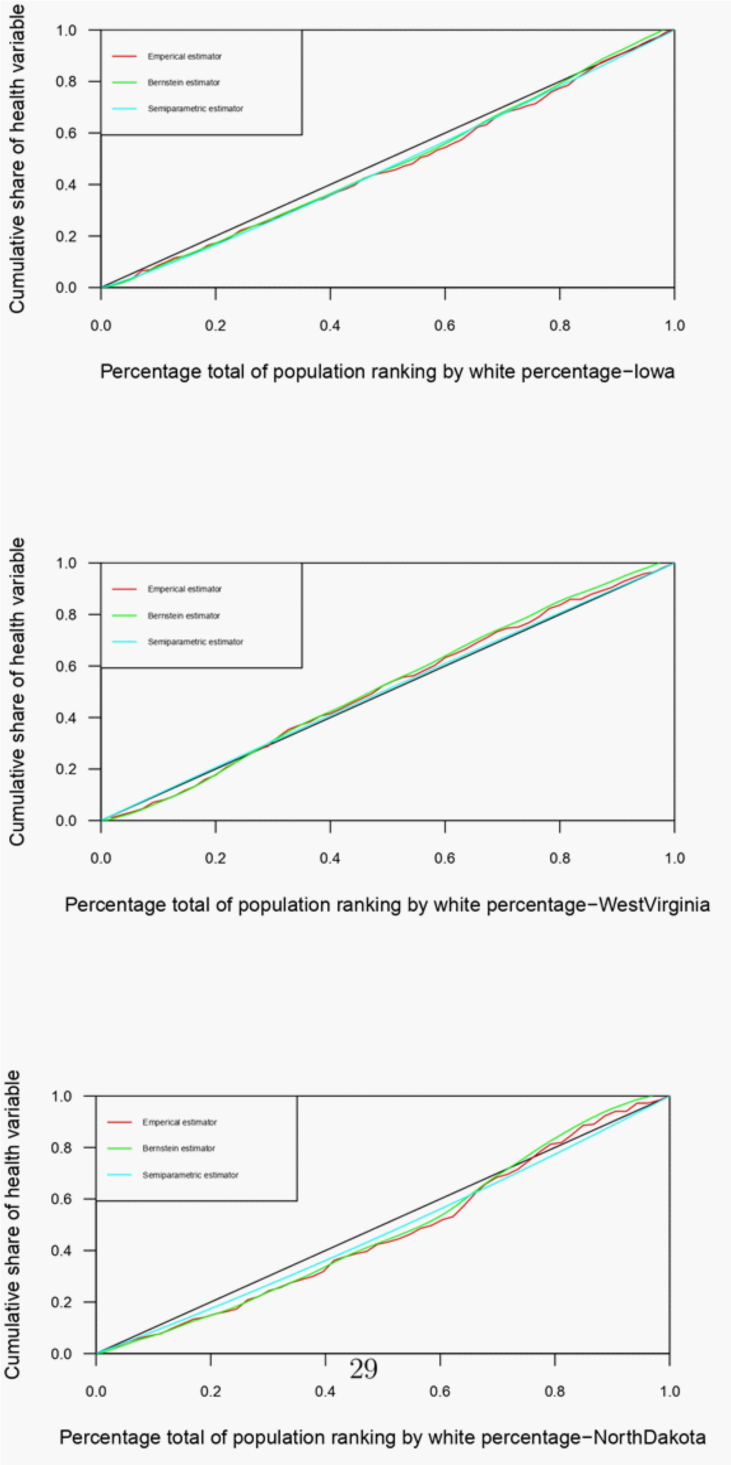

Figure 9: The empirical estimator, the semiparametric and the nonparametric estimator of the health concentration curve for COVID-19deaths. (high rate of white people states).

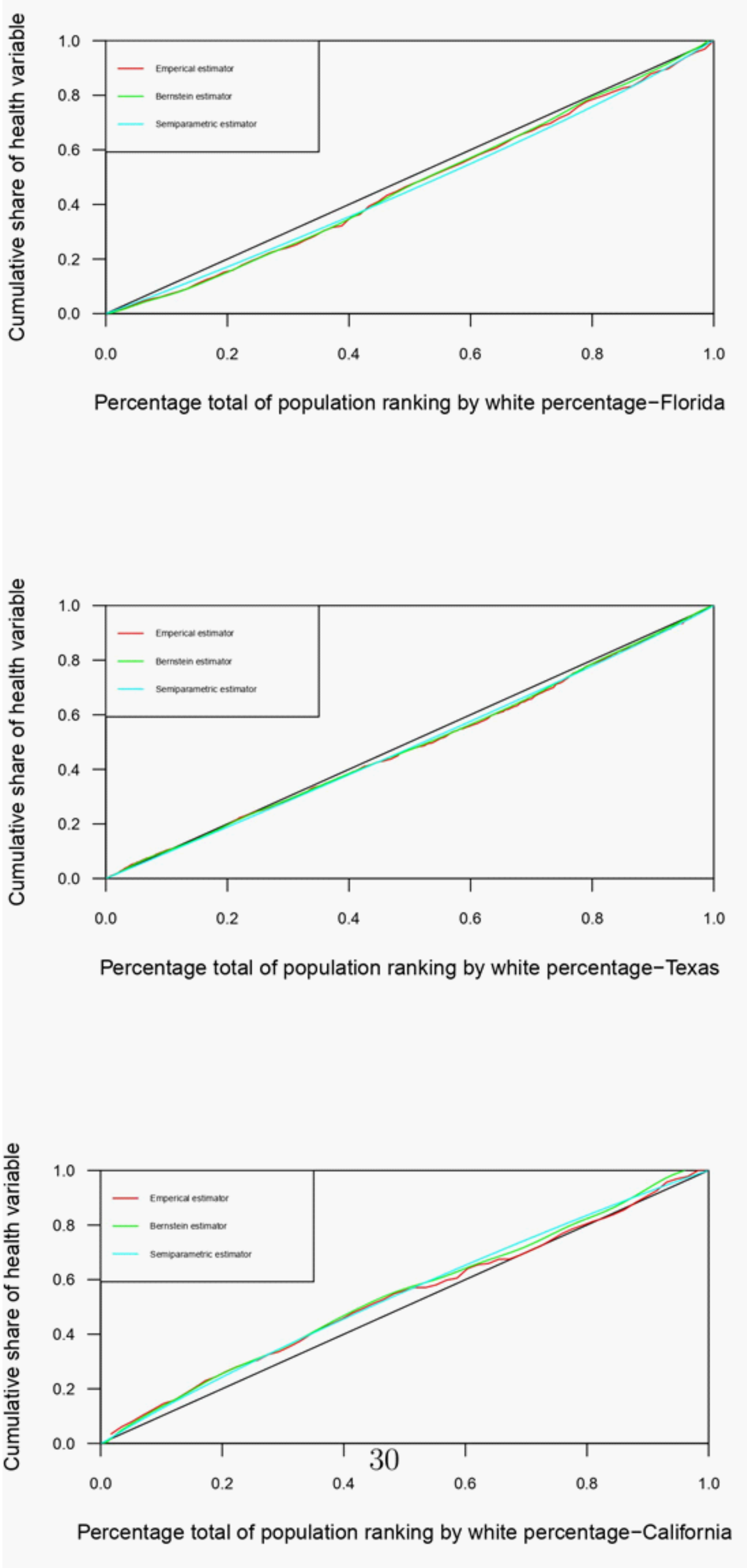

Figure 10: The empirical estimator, the semiparametric and the nonparametric estimator of the health concentration curve for COVID-19deaths. (low rate of white people states).

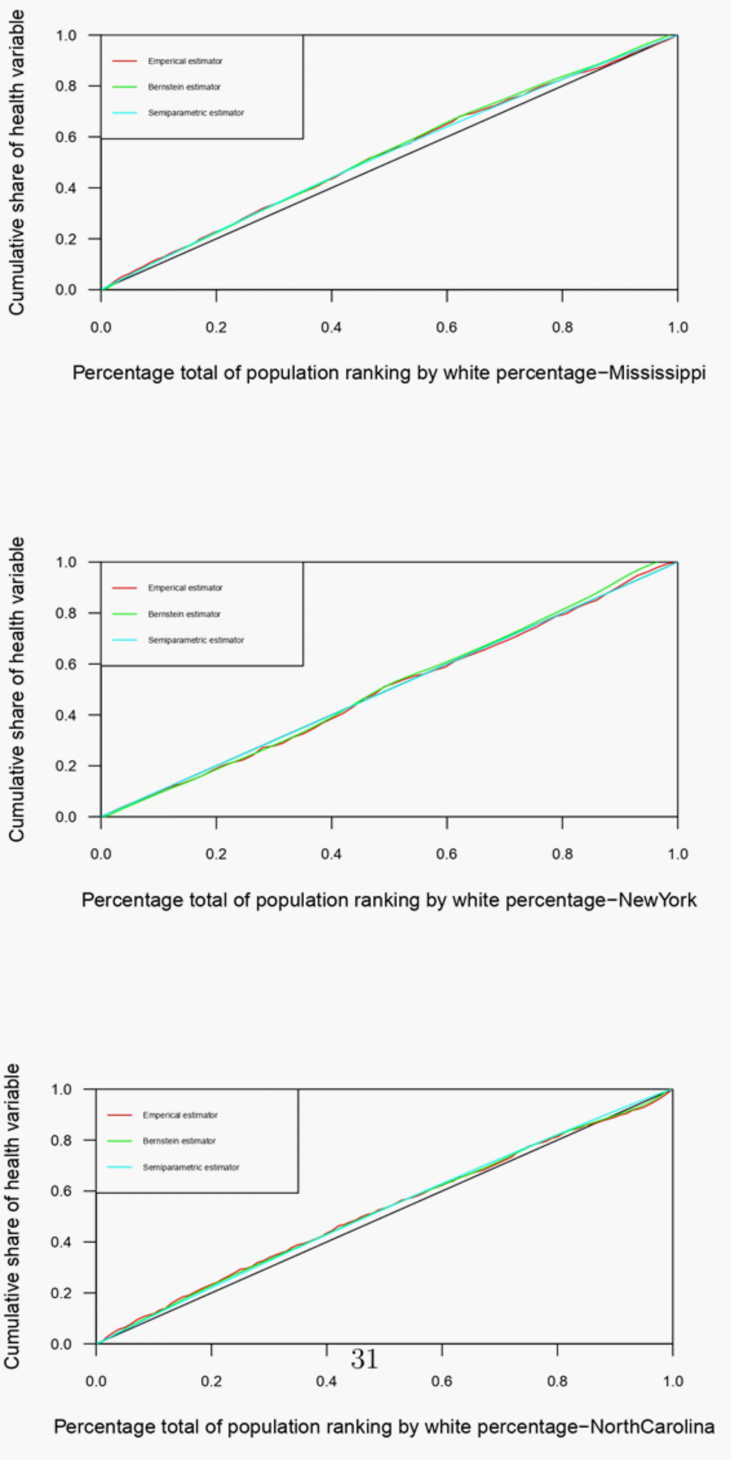

Figure 11: The empirical estimator, the semiparametric and the nonparametric estimator of the health concentration curve for COVID-19deaths. (average rate of white people states).